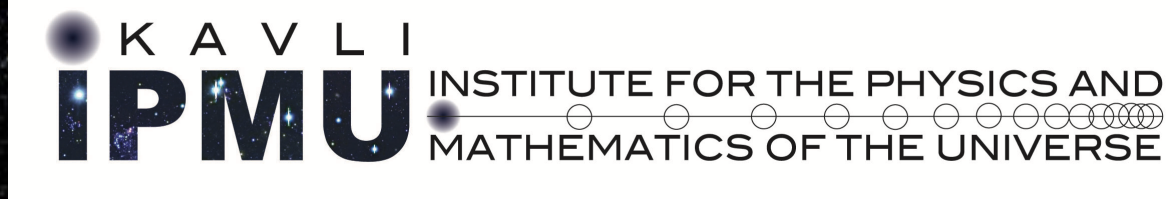


近傍矮小銀河で探る 暗黒物質の正体

林 航平、

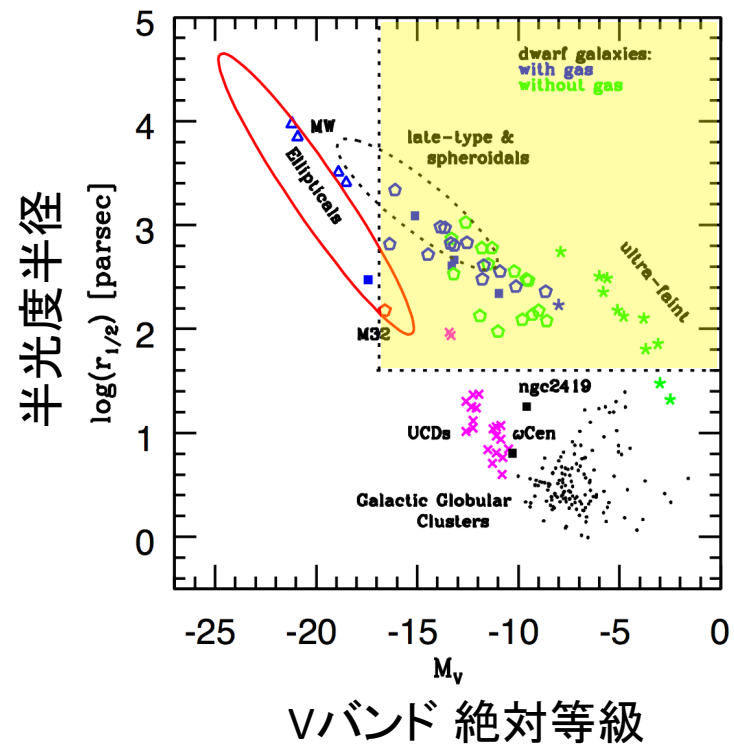
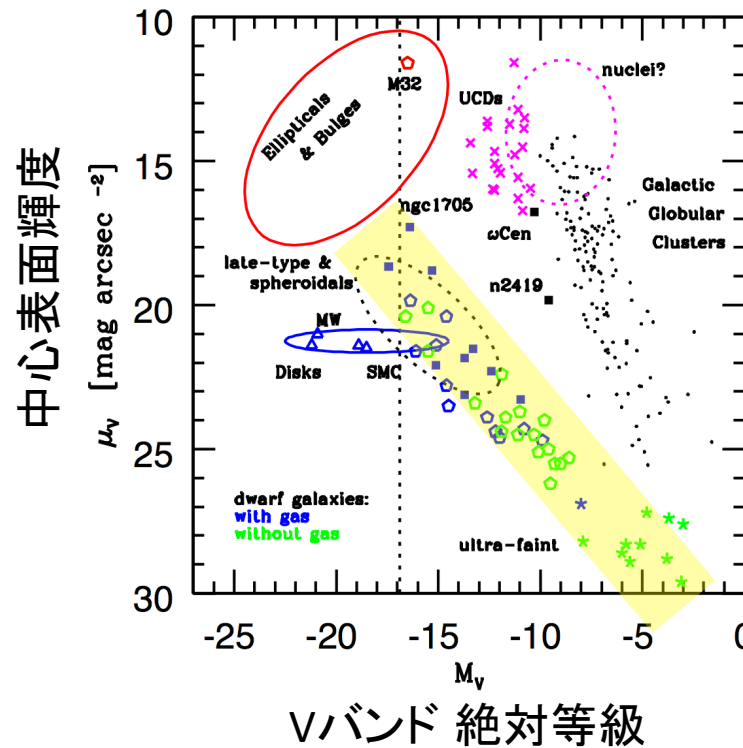
東京大学カブリIPMU
(JSPS研究員)



INTRODUCTION

Dwarf Spheroidal Galaxies

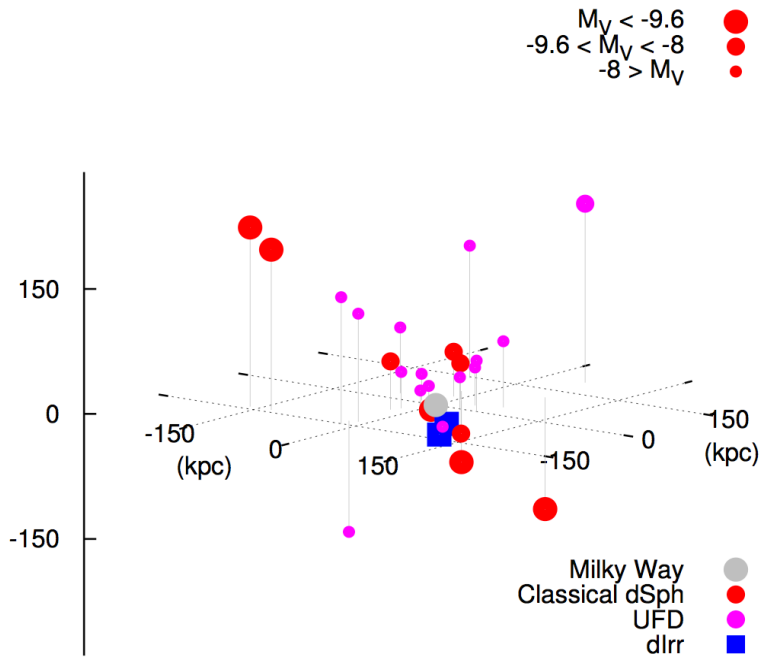
Structural properties for different types of galaxies



w/ gas = dwarf Irregulars (dIrr)
w/o gas = dwarf spheroidals (dSph), dwarf ellipticals (dE)

Tolstoy, Hill & Tosi 2009

Dwarf Spheroidal Galaxies



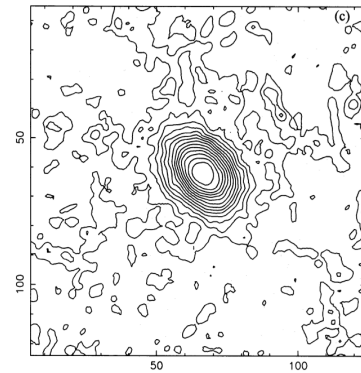
Basic Properties

- $M_V > -17$, $\mu_V > 20 \text{ mag arcsec}^{-2}$
- Half-light radius $\sim 100 - 1000 \text{ pc}$
- (almost) no gas and no current SF
- Non-spherical shape**
typical axial ratio 0.6 - 0.7 (MW)
0.7 - 0.9 (M31)

Fornax dSph



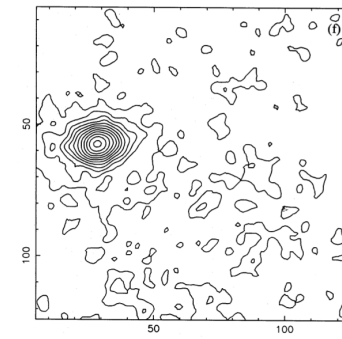
Irwin & Hatzidimitriou 1995



Projected axial ratio : 0.70 ± 0.01

Half-light radius (Plummer) : $668 \pm 34 \text{ pc}$

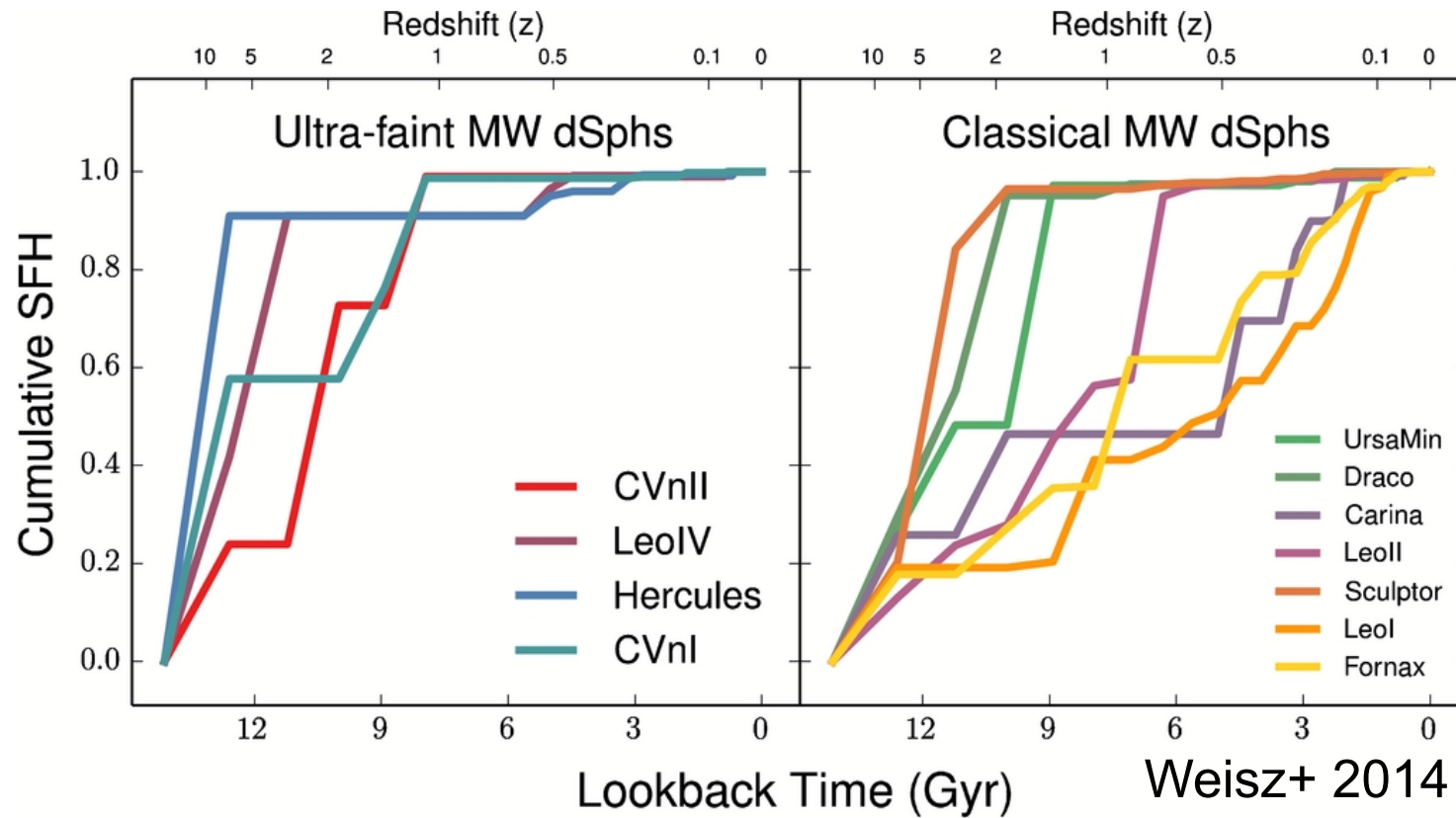
Sculptor dSph



Projected axial ratio : 0.68 ± 0.03

Half-light radius (Plummer) : $260 \pm 39 \text{ pc}$

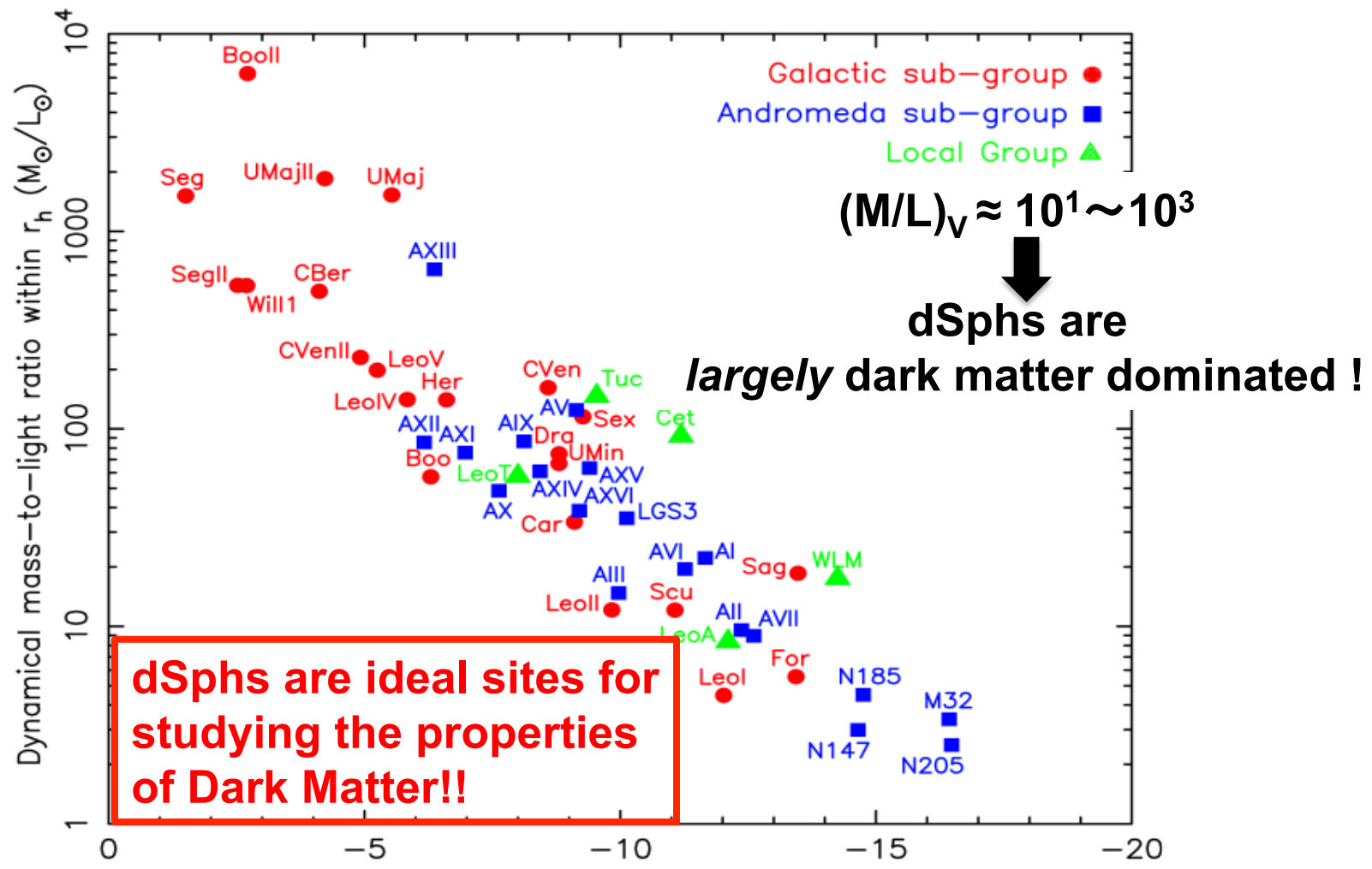
Star Formation Histories of dSphs



The brightest dSphs have **diverse formation histories** such as single, multiple burst and consecutive star formation.

Dynamical Properties of dSphs

Mass to Light ratio (M/L) within stellar extent in dSphs



Dark Matter Detection by Gamma-Ray

dSph galaxy



$$\frac{\Phi(E, \Delta\Omega)}{\text{Observed } \gamma\text{-Ray Flux}} = \left[\frac{\langle \sigma v \rangle}{8\pi m_{\text{DM}}^2} \sum_f \text{Br}(\text{DM DM} \rightarrow f) \left(\frac{dN_\gamma}{dE} \right) \right] \left[\int_{\Delta\Omega} d\Omega \int_{\text{l.o.s}} dl \rho^2(l, \Omega) \right]$$

Observed
γ-Ray Flux

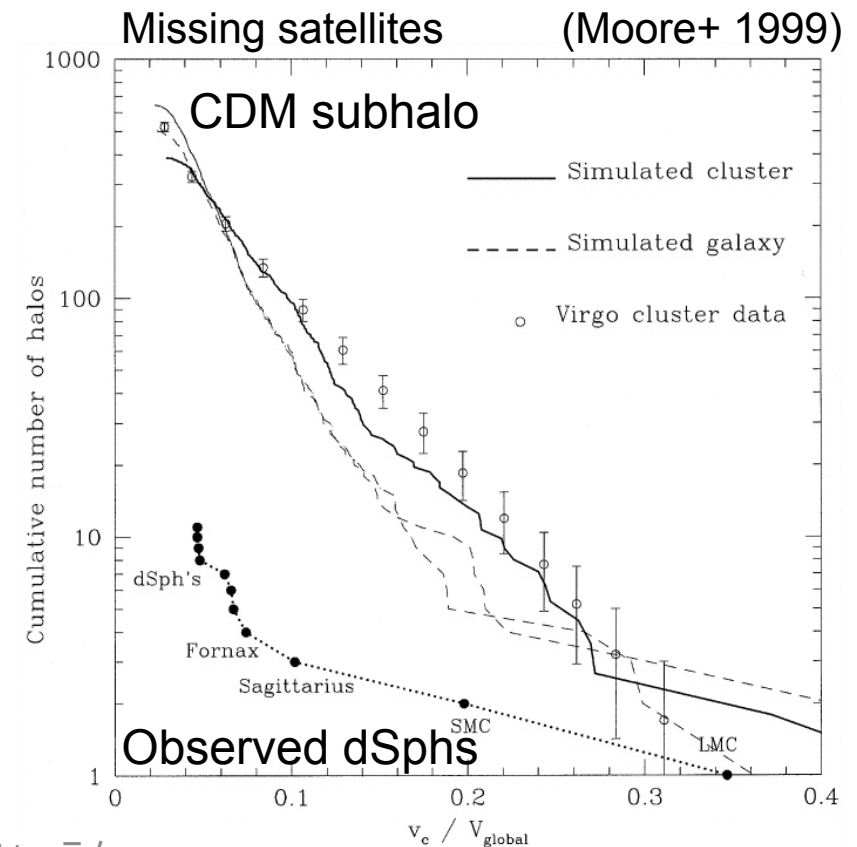
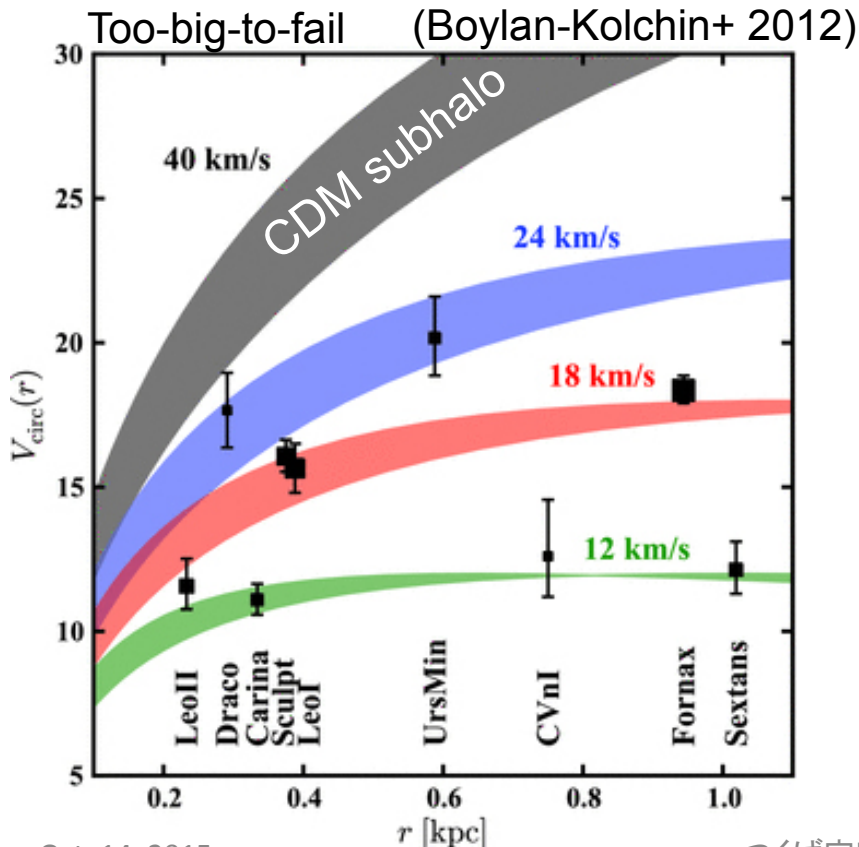
Theoretical prediction

Determination of J-factor is essential
to constrain the DM property

Halo Profile
(J-factor)

Λ CDM theory: small scale “crisis”

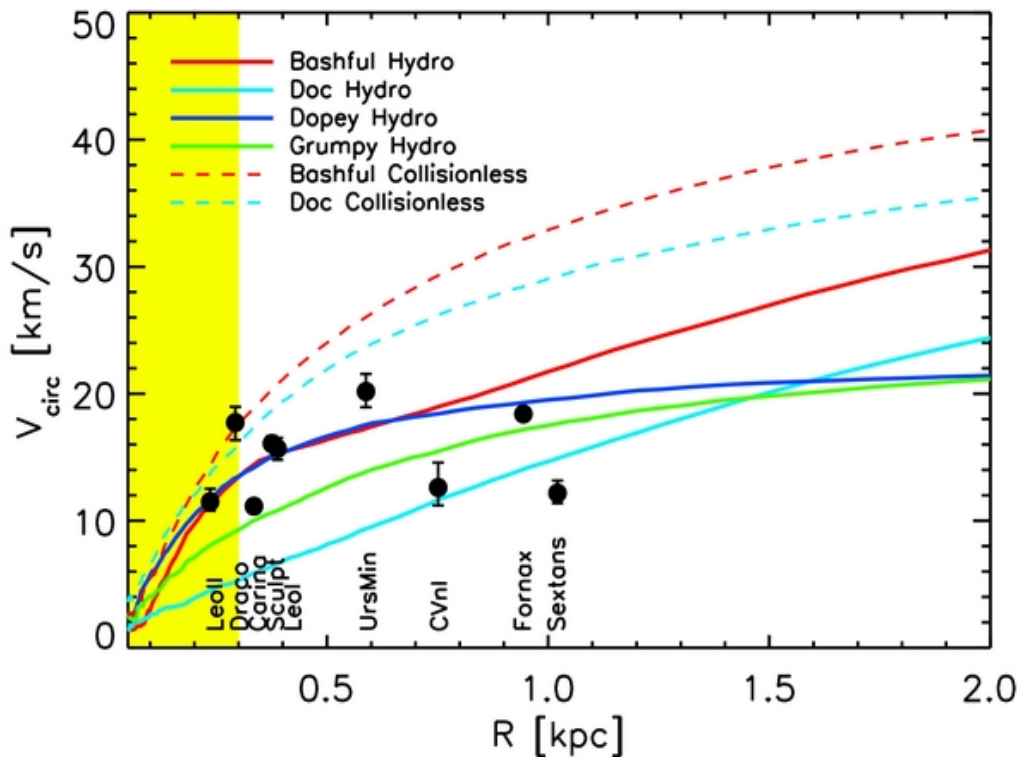
- Core-cusp problem (Burkert+ 1995, Gilmore+ 2007)
- Too-big-to-fail problem (Boylan-Kolchin+ 2012)
- Missing satellites problem (Moore+ 1999, Klypin+ 1999)



Λ CDM theory: Can baryons help it?

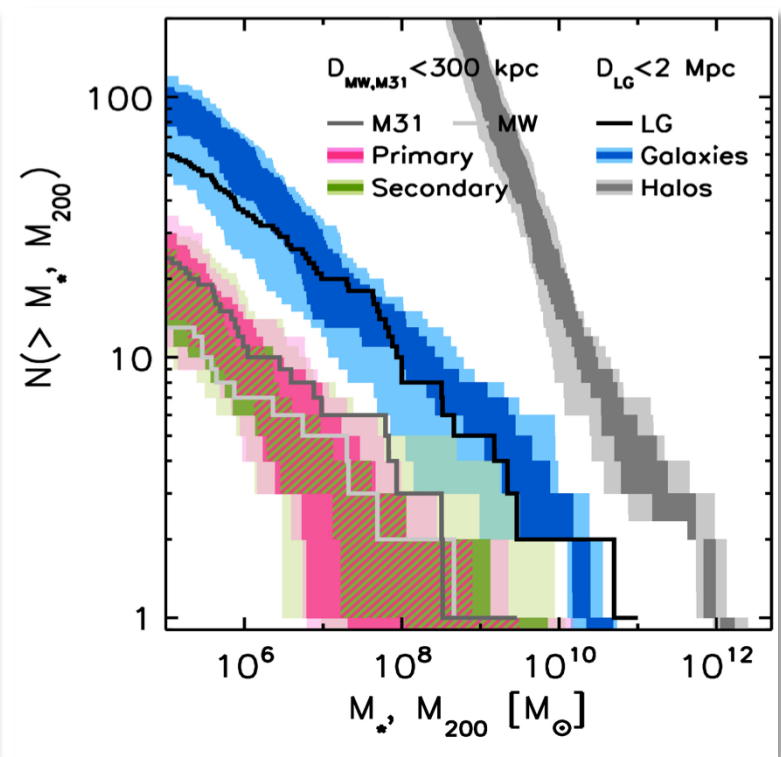
CDM + Baryon feedback + UV background

Too-big-to-fail



Madau+ 2014

Missing satellites

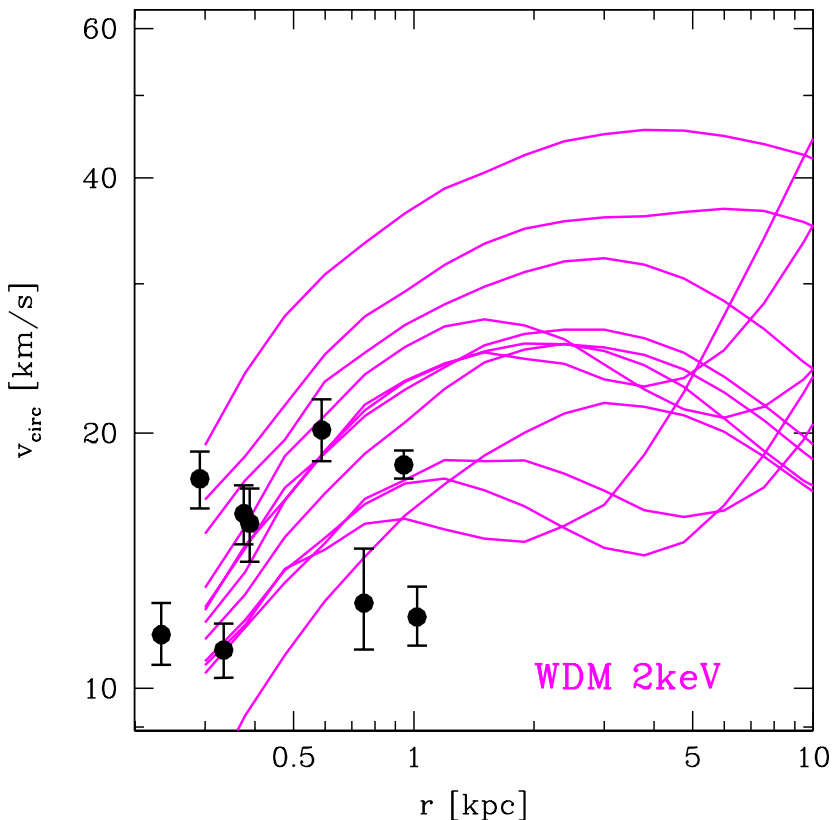


Sawala+ 2014

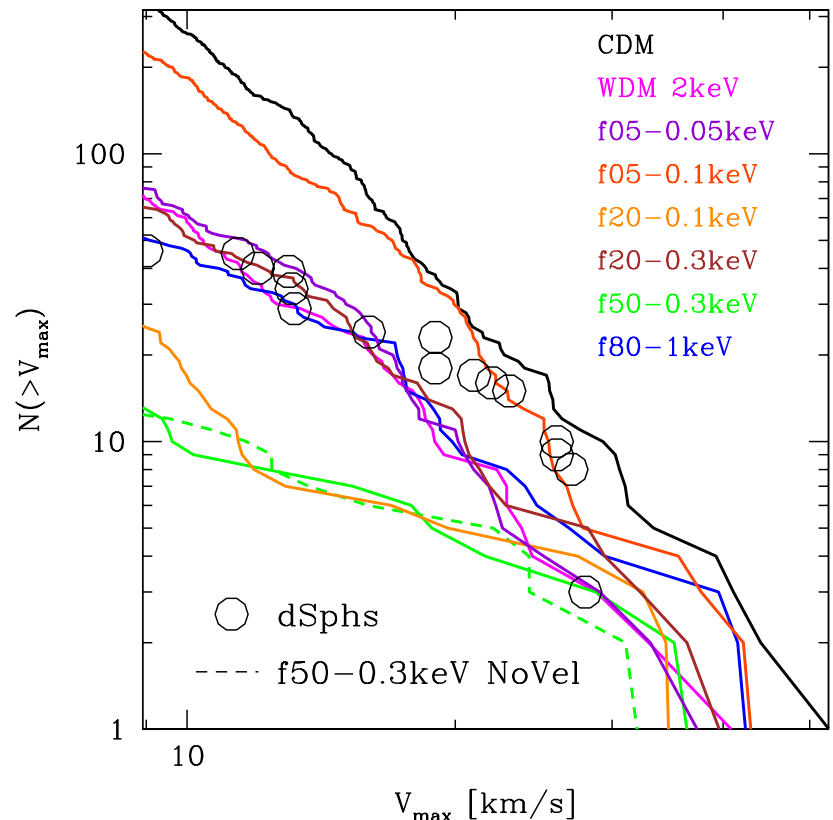
Λ CDM theory: Can Warm Dark Matter do it?

Warm Dark Matter (or Mixed Dark Matter)

Too-big-to-fail



Missing satellites



Anderhalden+ 2014

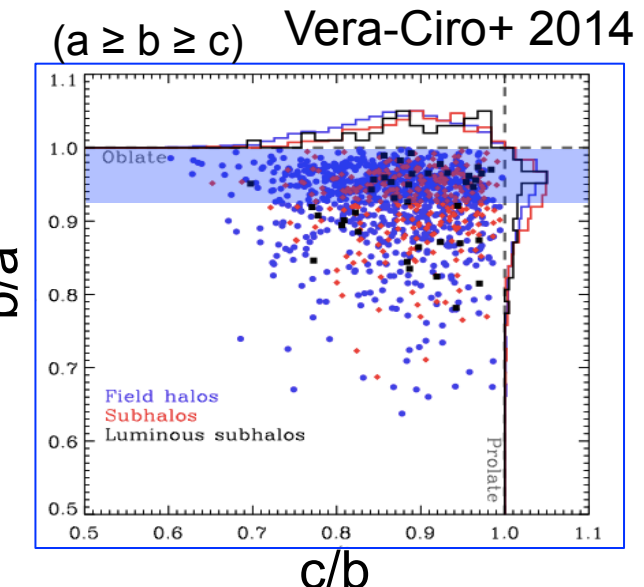
Oct. 14, 2015

つくば宇宙フォーラム

Λ CDM theory: further inspections

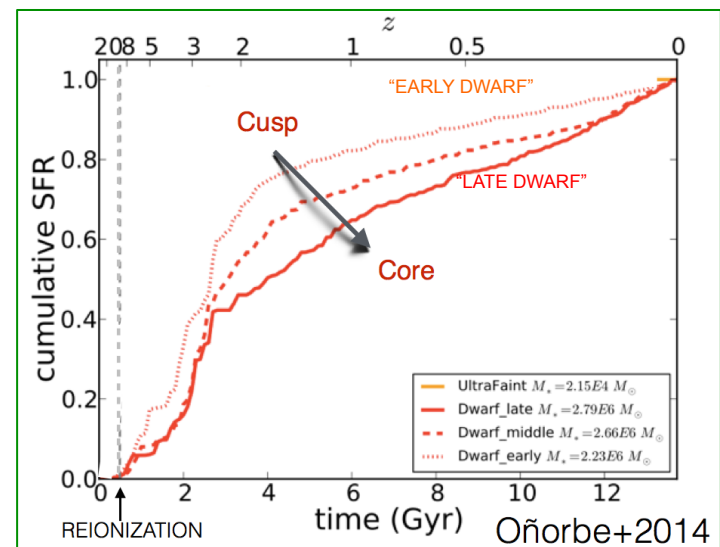
- Shapes of the dark halo in dSphs?

Recent N-body simulations have predicted that dark subhalos are not strongly triaxial, but rather statistically oblate, axisymmetric shapes.



- Is there a link between dark and luminous components?

In the light of suggestions from N-body simulations, dark halo structures can be related with the evolution of less massive galaxies such as star formation history and chemical enrichment.



The purpose of my study

Motivation

is to obtain more realistic and reliable limits on the non-spherical density structure of dark halos and to investigate their dark matter properties in more detail.

To do this,

we construct axisymmetric mass models with velocity anisotropy in the stellar system for dSphs in the MW and M31.

MODEL AND DATA

※Assumptions※

- Stellar components are in dynamical equilibrium.
- Static gravitational potential is dominated by DM.
- DSphs are considered as a collisionless system.
- Axisymmetry in both stellar and DM components.
- Velocity anisotropy, β_z , is constant.

• Axisymmetric Jeans equations

$$\overline{v_z^2} = \frac{1}{\nu(R, z)} \int_z^\infty \nu \frac{\partial \Phi}{\partial z} dz \quad \overline{v_\phi^2} = \frac{1}{1 - \beta_z} \left[\overline{v_z^2} + \frac{R}{\nu} \frac{\partial(\nu \overline{v_z^2})}{\partial R} \right] + R \frac{\partial \Phi}{\partial R}$$

$$\beta_z = 1 - \overline{v_z^2}/\overline{v_R^2} \quad : \text{velocity anisotropy}$$

• Luminous component

$$\nu(R, z) = \frac{3L}{4\pi b_*^3} \left[1 + \frac{m_*^2}{b_*^2} \right]^{-5/2}$$

$$m_*^2 = R^2 + \frac{z^2}{q^2} \quad q : \text{axial ratio}$$

$$q'^2 = \cos^2 i + q^2 \sin^2 i \quad q' : \text{projected } q$$

• DM-halo component

$$\rho(R, z) = \rho_0 \left(\frac{m}{b_{\text{halo}}} \right)^\alpha \left[1 + \left(\frac{m}{b_{\text{halo}}} \right)^2 \right]^{-(\alpha+3)/2}$$

$$m^2 = R^2 + \frac{z^2}{Q^2} \quad Q : \text{DM's axial ratio}$$

※Assumptions※

- Stellar components are in dynamical equilibrium.
- Static gravitational potential is dominated by DM.
- DSphs are considered as a collisionless system.
- Axisymmetry in both stellar and DM components.
- Velocity anisotropy, β_z , is constant.

Axisymmetric Jeans equations

$$\bar{v}_z^2 = \frac{1}{\nu(R, z)} \int_z^\infty \nu \frac{\partial \Phi}{\partial z} dz \quad \bar{v}_\phi^2 = \frac{1}{1 - \beta_z} \left[\bar{v}_z^2 + R \frac{\partial(\nu \bar{v}_z^2)}{\partial R} \right] + R \frac{\partial \Phi}{\partial R}$$

$\beta_z = 1 - \bar{v}_z^2 / \bar{v}_R^2$: velocity anisotropy

Free parameters

Luminous component

$$\nu(R, z) = \frac{3L}{4\pi b_*^3} \left[1 + \frac{m_*^2}{b_*^2} \right]^{-5/2}$$

$$m_*^2 = R^2 + \frac{z^2}{q^2} \quad q : \text{axial ratio}$$

$$q'^2 = \cos^2 i + q^2 \sin^2 i \quad q' : \text{projected } q$$

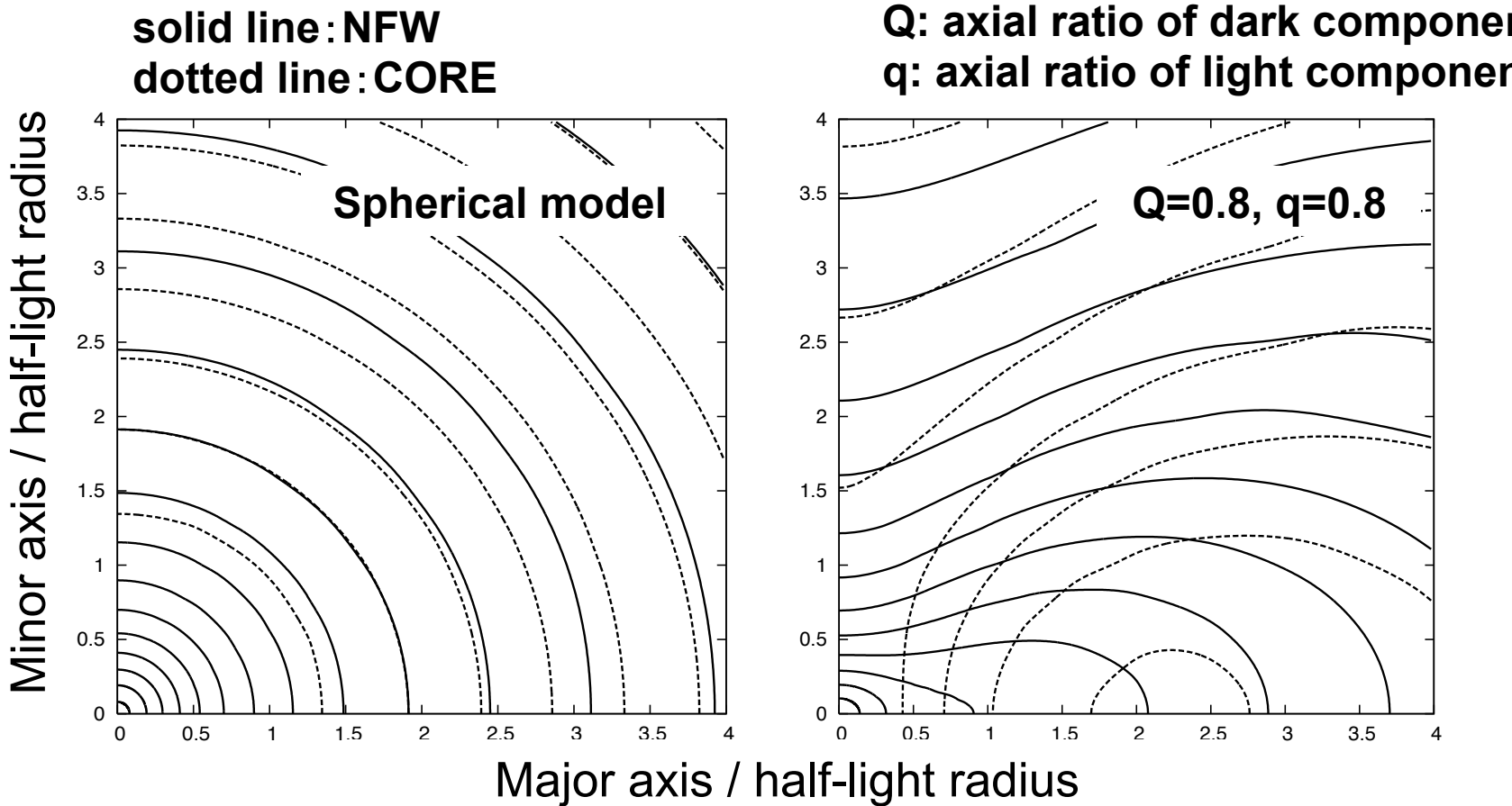
DM-halo component

$$\rho(R, z) = \rho_0 \left(\frac{m}{b_{\text{halo}}} \right)^\alpha \left[1 + \left(\frac{m}{b_{\text{halo}}} \right)^2 \right]^{-(\alpha+3)/2}$$

$$m^2 = R^2 + \frac{z^2}{Q^2} \quad Q : \text{DM's axial ratio}$$

2D map of I-o-s velocity dispersion

A non-spherical dark matter distribution can be deduced from such characteristic distributions of stellar kinematics.



The observational dataset

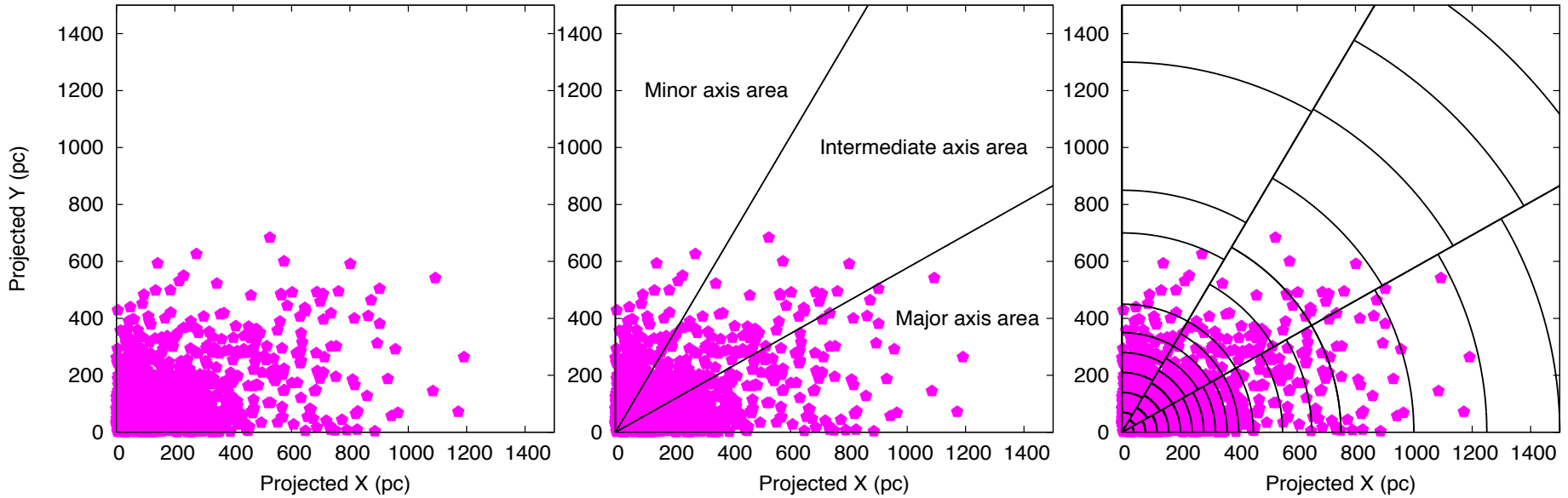
Table 1. The observational dataset for MW and M31 dSph satellites

Object	No. of stars	M_* ($10^6 M_\odot$)	M_V	D_\odot (kpc)	r_{half} (pc)	q' (axial ratio)	$\tau_{0.7}^{\text{a}}$ (Gyr)	Ref. ^b
MW dSphs								
Carina	776	0.38	-9.1 ± 0.5	106 ± 6	241 ± 23	0.67 ± 0.05	4.5	1,3,7
Fornax	2523	20.0	-13.4 ± 0.3	147 ± 12	668 ± 34	0.70 ± 0.01	4.6	1,3,7
Sculptor	1360	2.3	-11.1 ± 0.5	86 ± 6	260 ± 39	0.68 ± 0.03	12.7	1,3,7
Sextans	445	0.44	-9.3 ± 0.5	86 ± 4	682 ± 117	0.65 ± 0.05	No data	1,3,7
Draco	185	0.29	-8.8 ± 0.3	76 ± 6	196 ± 12	0.69 ± 0.02	11.5	2,7
Leo I	328	5.5	-12.0 ± 0.3	254 ± 15	246 ± 19	0.79 ± 0.03	2.7	2,3,7
Leo II	200	0.74	-9.8 ± 0.3	233 ± 14	151 ± 17	0.87 ± 0.05	6.8	1,7
M31 dSphs								
And I	51	3.9	-11.7 ± 0.1	745 ± 24	670 ± 30	0.78 ± 0.04	7.6	5,6,7
And II	488	7.6	-12.4 ± 0.2	652 ± 18	1230 ± 20	0.90 ± 0.02	6.2	4,6,7
And III	62	0.83	-10.0 ± 0.3	748 ± 24	400 ± 30	0.48 ± 0.02	8.8	5,6,7
And V	85	0.39	-9.1 ± 0.2	773 ± 28	350 ± 20	0.82 ± 0.05	10.0	5,6,7
And VII	136	9.5	-12.6 ± 0.3	762 ± 35	770 ± 20	0.87 ± 0.04	12.8	5,6,7

^aThis value is the lookback time at achieving 70% of current stellar mass of dSphs, and is estimated by available data taken from Weisz et al. (2014).

^bReferences: (1) Irwin & Hatzidimitriou (1995); (2) Martin et al. (2008); (3) Walker et al. (2009c); (4) Ho et al. (2012); (5) Tollerud et al. (2012); (6)McConnachie & Irwin (2006); (7) McConnachie (2012)

The observational dataset



Fitting method: MCMC technique

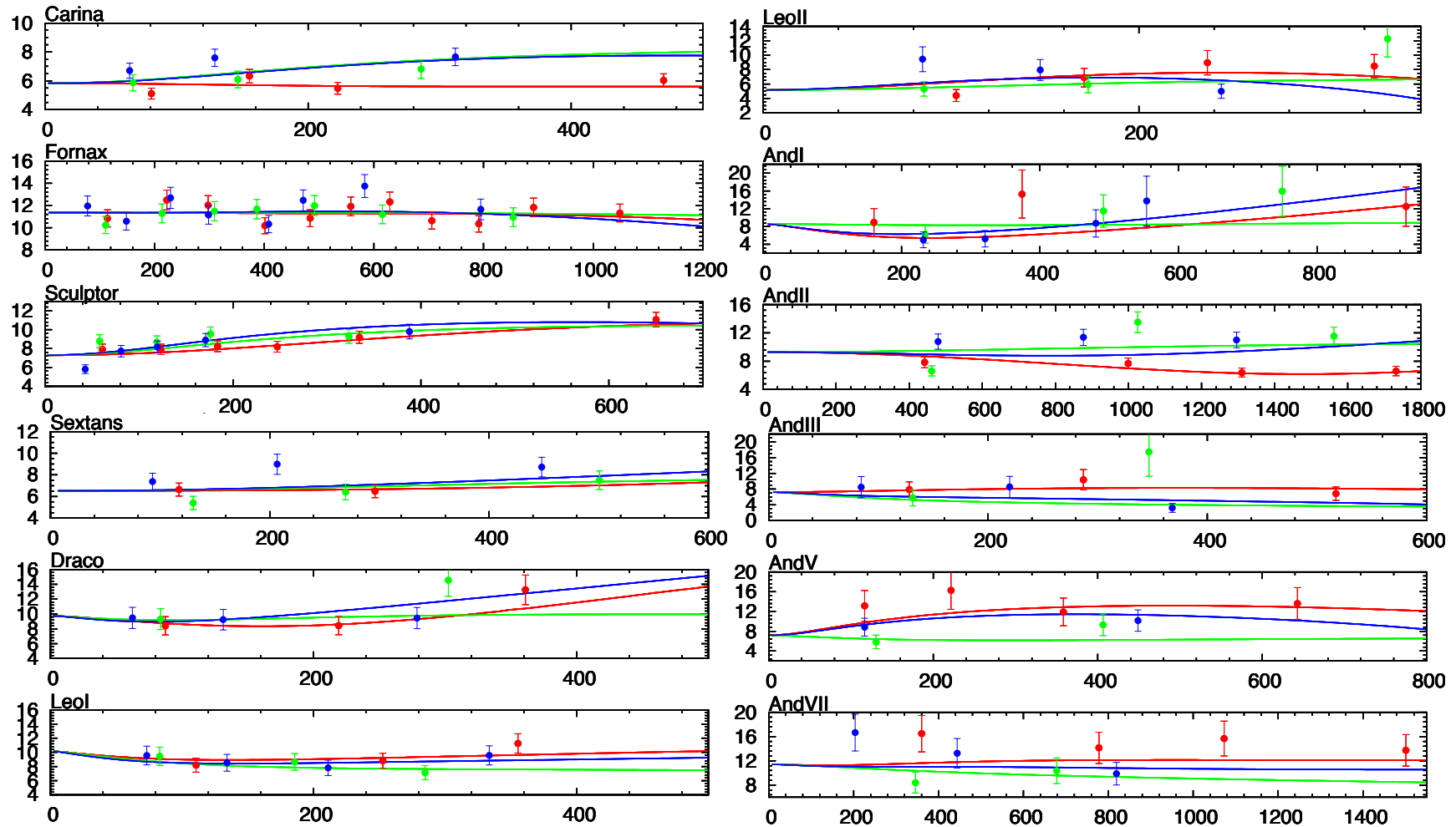
$$P_i(\sigma_{\text{los},i} | \mathbf{M}) = \frac{1}{\sqrt{2\pi \text{Var}(\sigma_{\text{los},i})}} \exp \left[-\frac{1}{2} \frac{(\sigma_{\text{los},i} - \sigma_{t,i})^2}{\text{Var}(\sigma_{\text{los},i})} \right]$$

$$\mathbf{M} = (Q, b_{\text{halo}}, \rho_0, \beta_z, \alpha, i)$$

RESULTS

Line-of-sight velocity dispersion profile

L-o-s velocity dispersion (km/s)



Major axis, Minor axis, intermediate axis (pc)

Best-fit parameters

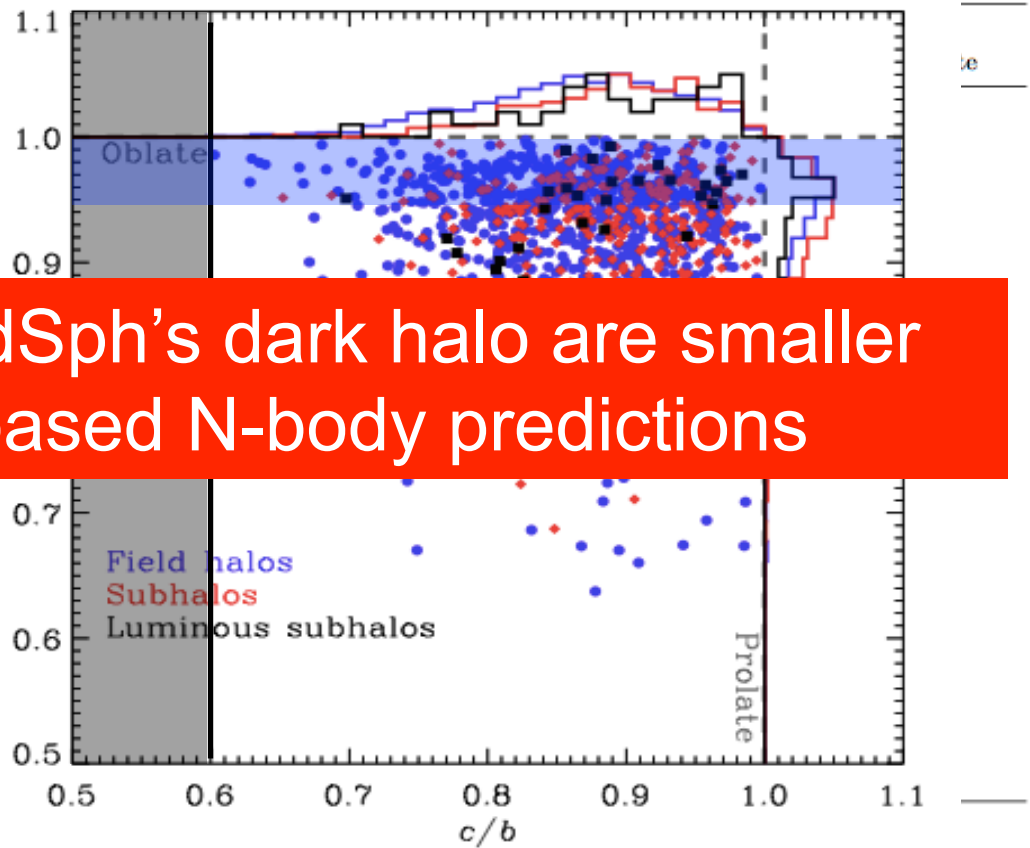
Table 2. Results of MCMC analysis for twelve dSph galaxies.

Galaxy	Q	$b_{\text{halo}} [\text{pc}]$	$\rho_0 [\text{M}_\odot \text{ pc}^{-3}]$	β_z	α	$i [\text{deg}]$
MW dSphs						
Carina	0.33 ± 0.02	$709.7^{+40.6}_{-44.3}$	0.107 ± 0.006	-0.05 ± 0.06	$-0.09^{+0.09}_{-0.05}$	$87.1^{+2.9}_{-9.1}$
Fornax	0.38 ± 0.03	$991.1^{+27.0}_{-21.4}$	0.086 ± 0.003	$-0.17^{+0.16}_{-0.07}$	$0.00_{-0.04}$	$90.0_{-10.6}$
Sculptor	0.45 ± 0.03	$637.7^{+32.6}_{-26.0}$	0.168 ± 0.008	$-0.03^{+0.06}_{-0.04}$	$0.00_{-0.09}$	$87.8^{+2.2}_{-9.1}$
Sextans	0.53 ± 0.06	$1126.7^{+93.5}_{-74.5}$	0.028 ± 0.008	$0.23^{+0.12}_{-0.18}$	$0.00_{-0.10}$	$89.8^{+0.2}_{-12.5}$
Draco	0.40 ± 0.05	$590.2^{+46.5}_{-43.9}$	0.153 ± 0.021	$0.31^{+0.08}_{-0.13}$	$-0.86^{+0.11}_{-0.11}$	$75.6^{+14.4}_{-8.8}$
Leo I	0.86 ± 0.10	$581.8^{+33.3}_{-26.1}$	0.037 ± 0.005	0.09 ± 0.14	$-1.40^{+0.06}_{-0.08}$	$70.5^{+19.5}_{-7.5}$
Leo II	0.91 ± 0.16	$281.8^{+35.3}_{-30.6}$	0.195 ± 0.031	$-0.62^{+0.56}_{-1.8}$	$0.00_{-0.11}$	$88.8^{+0.2}_{-34.3}$
M31 dSphs						
And I	$2.41^{+0.49}_{-0.39}$	$811.3^{+118.1}_{-112.7}$	0.037 ± 0.009	$0.79^{+0.03}_{-0.05}$	$-0.39^{+0.39}_{-0.29}$	$90.0_{-34.8}$
And II	0.57 ± 0.04	$2290.9^{+174.8}_{-84.1}$	0.010 ± 0.002	$0.22^{+0.05}_{-0.06}$	$0.00_{-0.04}$	$89.9^{+0.1}_{-15.6}$
And III	0.16 ± 0.04	$796.9^{+90.5}_{-96.8}$	0.043 ± 0.01	≤ -0.21	$-1.43^{+0.14}_{-0.23}$	$70.8^{+8.6}_{-3.3}$
And V	$4.75^{+4.54}_{-1.71}$	$369.9^{+35.6}_{-37.2}$	0.039 ± 0.007	≤ 0.13	$-1.33^{+0.21}_{-0.12}$	$78.2^{+11.8}_{-14.3}$
And VII	1.60 ± 0.39	$486.6^{+40.3}_{-28.8}$	0.062 ± 0.01	$0.12^{+0.19}_{-0.47}$	$-0.35^{+0.20}_{-0.46}$	$75.4^{+14.6}_{-18.6}$

Best-fit parameters

Table 2. Results of MCMC analysis for twelve dSph galaxies.

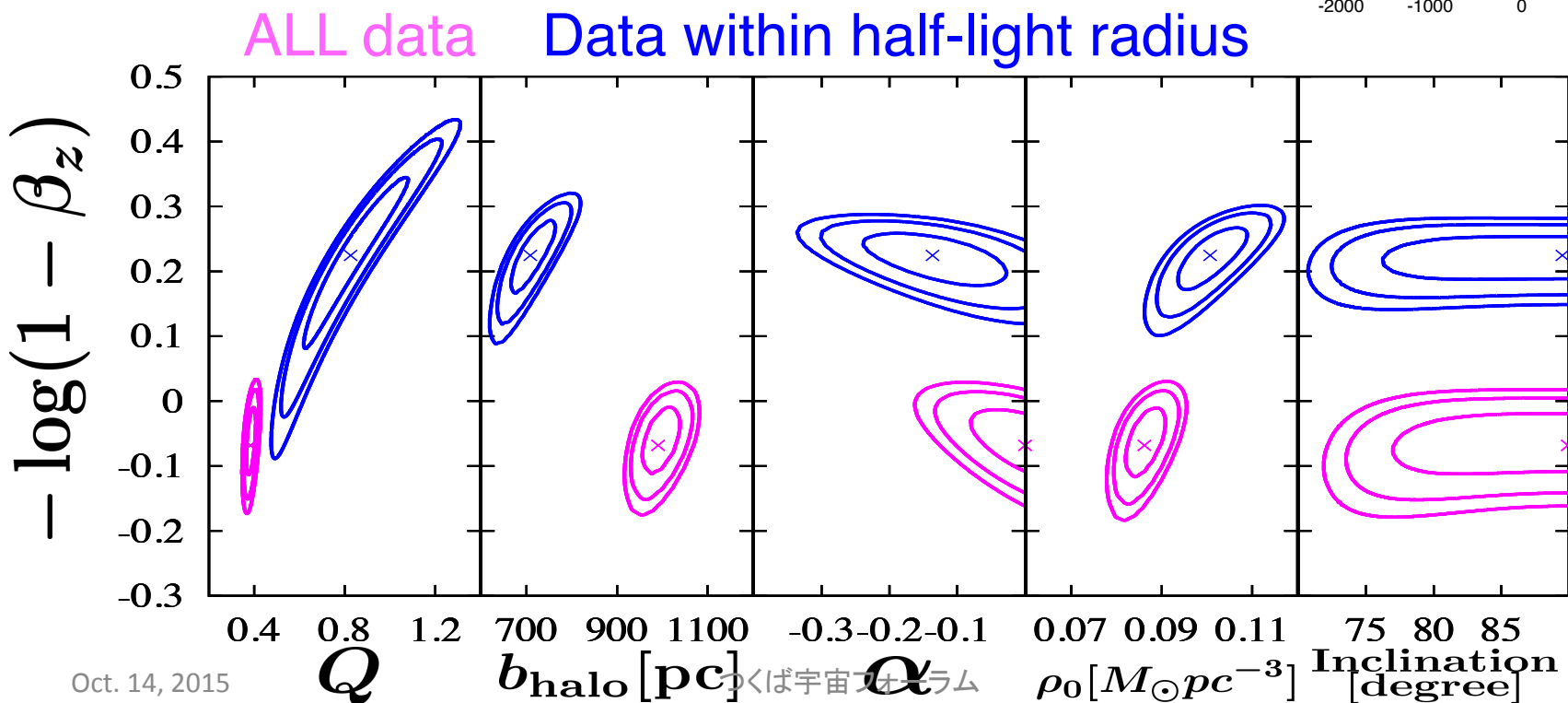
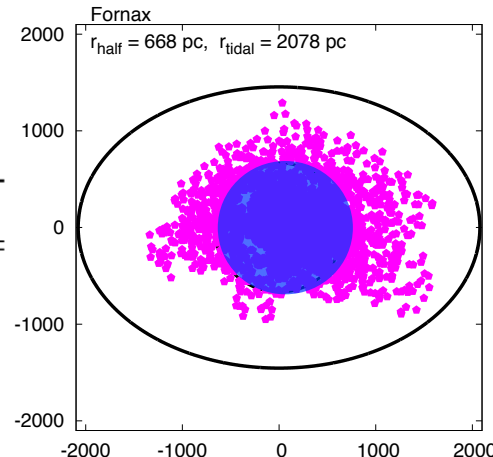
Galaxy	Q	$b_{\text{halo}} [\text{pc}]$
MW dSphs		
Carina	0.33 ± 0.02	$709.7^{+40.6}_{-44.3}$
Fornax	0.38 ± 0.03	$991.1^{+27.0}_{-21.4}$
Sculptor	0.45 ± 0.02	$627.7^{+32.6}_{-32.6}$
ECC II	0.01 ± 0.10	$2010.0^{+30.6}_{-30.6}$
M31 dSphs		
And I	$2.41^{+0.49}_{-0.39}$	$811.3^{+118.1}_{-112.7}$
And II	0.57 ± 0.04	$2290.9^{+174.8}_{-84.1}$
And III	0.16 ± 0.04	$796.9^{+90.5}_{-96.8}$
And V	$4.75^{+4.54}_{-1.71}$	$369.9^{+35.6}_{-37.2}$
And VII	1.60 ± 0.39	$486.6^{+40.3}_{-28.8}$



The impact of sample selection

Data volume and distribution of member stars

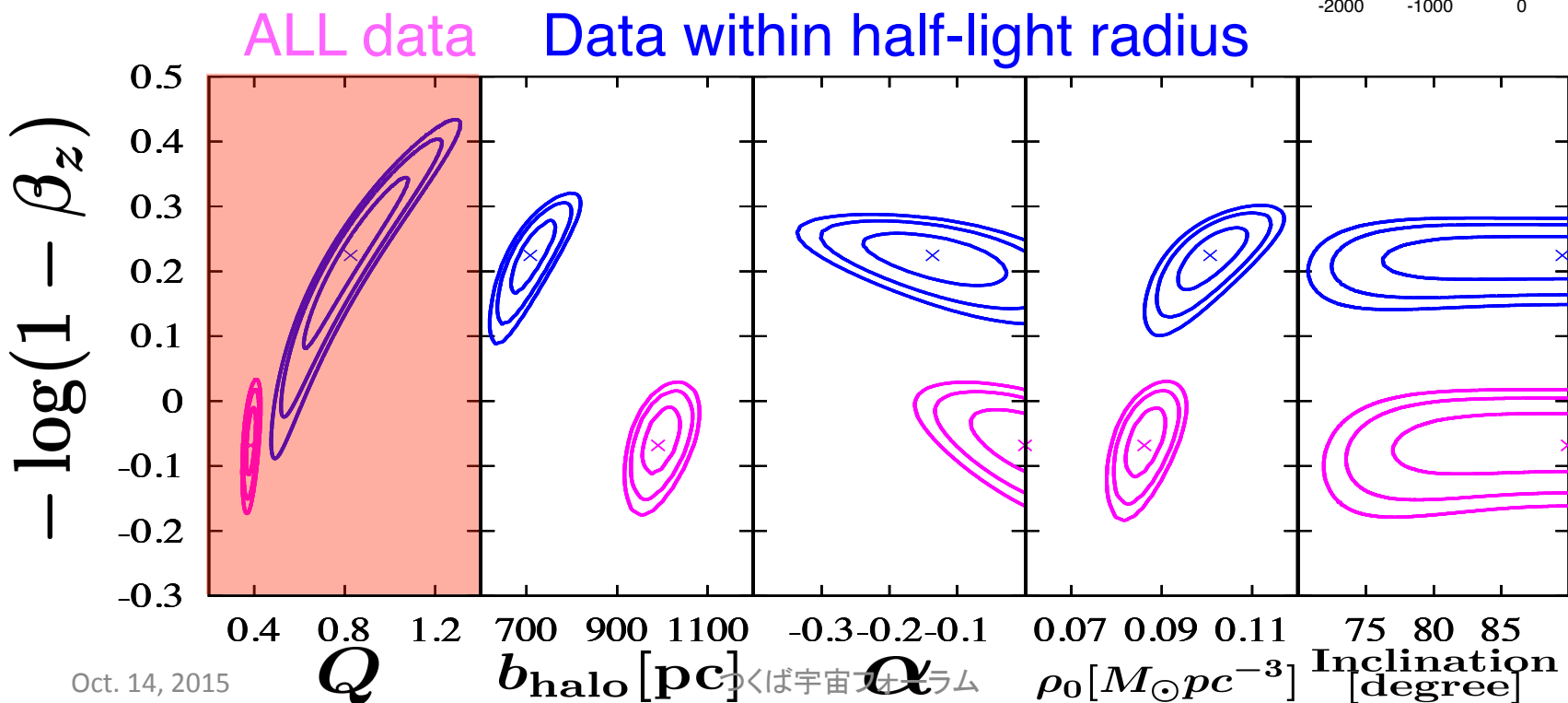
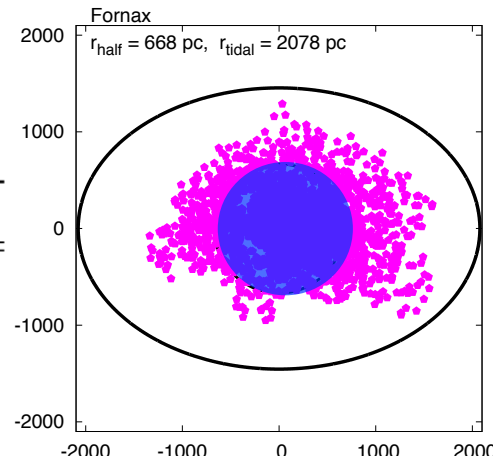
Object	Data	Q	$b_{\text{halo}} [\text{pc}]$	$\rho_0 [\text{M}_\odot \text{ pc}^{-3}]$	β_z	α	$i [\text{deg}]$
Fornax	Data within r_{half}	0.83 ± 0.04	$708.5^{+23.1}_{-16.7}$	0.101 ± 0.004	0.40 ± 0.03	-0.14 ± 0.06	$89.5^{+0.5}_{-10.6}$
	Full data	0.38 ± 0.03	$991.1^{+27.0}_{-21.4}$	0.086 ± 0.003	$-0.17^{+0.16}_{-0.07}$	$0.00_{-0.04}$	$90.0_{-10.6}$



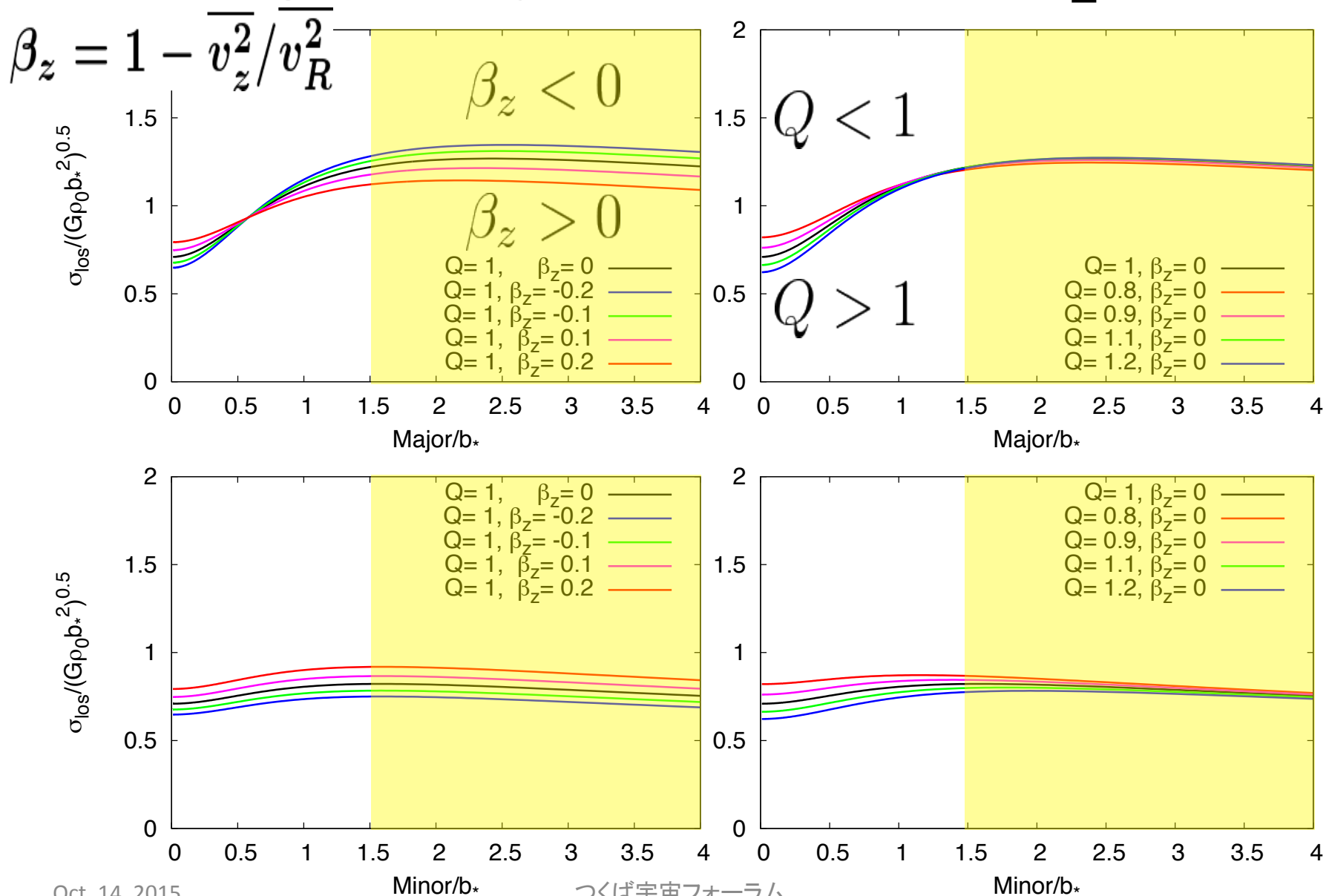
The impact of sample selection

Data volume and distribution of member stars

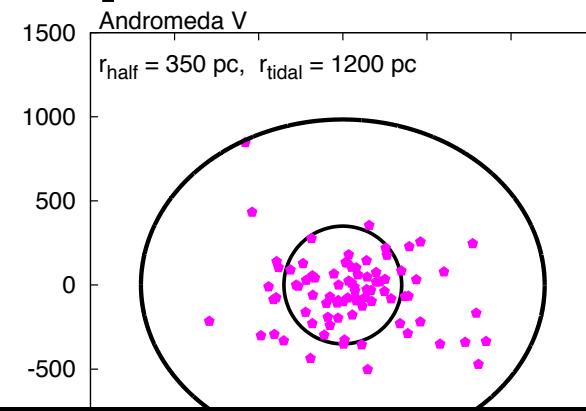
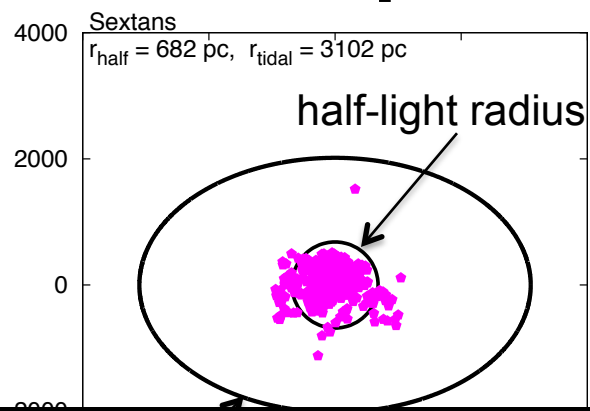
Object	Data	Q	$b_{\text{halo}} [\text{pc}]$	$\rho_0 [\text{M}_\odot \text{ pc}^{-3}]$	β_z	α	$i [\text{deg}]$
Fornax	Data within r_{half}	0.83 ± 0.04	$708.5^{+23.1}_{-16.7}$	0.101 ± 0.004	0.40 ± 0.03	-0.14 ± 0.06	$89.5^{+0.5}_{-10.6}$
	Full data	0.38 ± 0.03	$991.1^{+27.0}_{-21.4}$	0.086 ± 0.003	$-0.17^{+0.16}_{-0.07}$	$0.00_{-0.04}$	$90.0_{-10.6}$



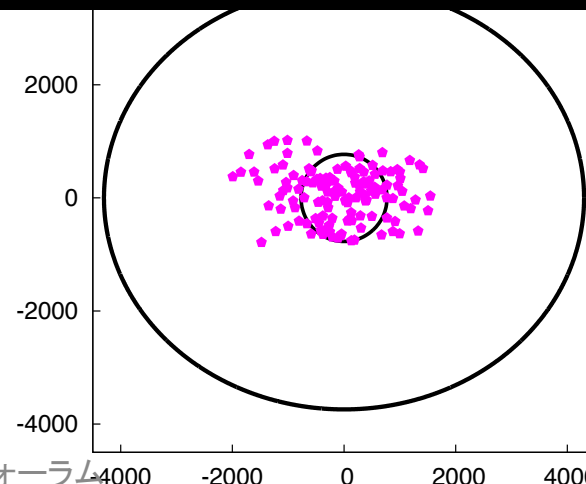
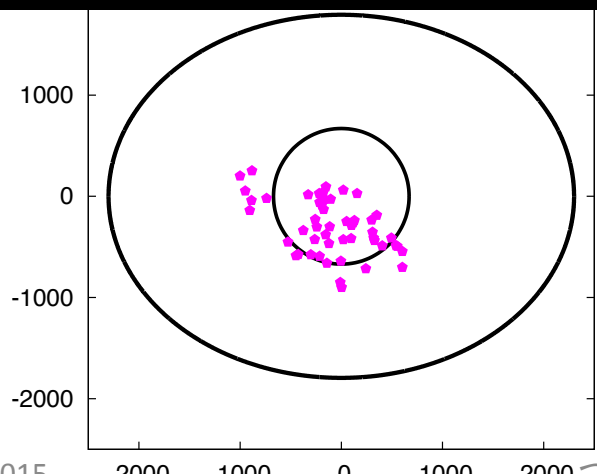
Degeneracy between Q and β_z ...



The impact of sample selection



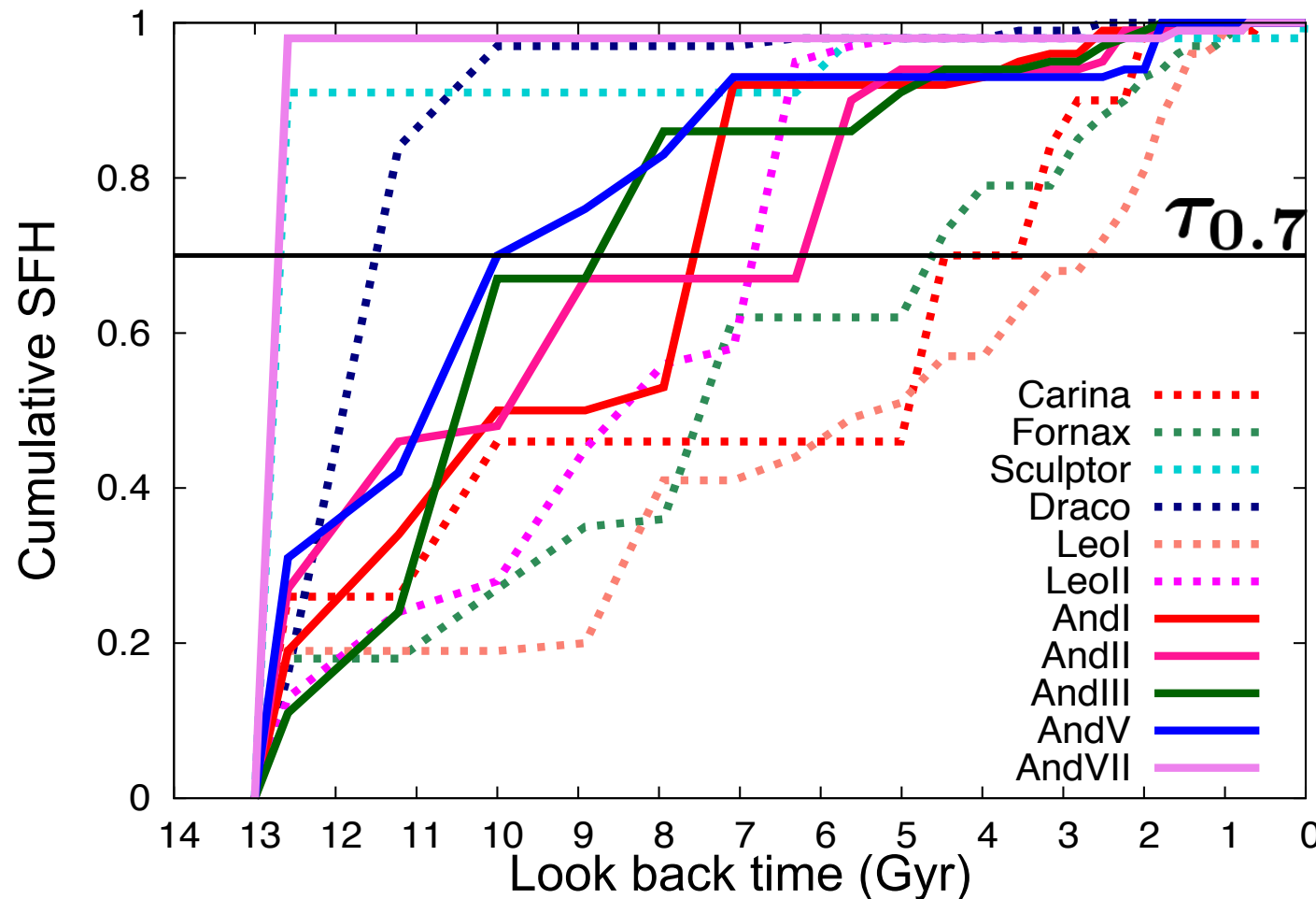
Require the observational data
over much larger areas



DISCUSSION

THE POSSIBLE LINK BETWEEN DARK-HALO STRUCTURE AND STAR-FORMATION HISTORY

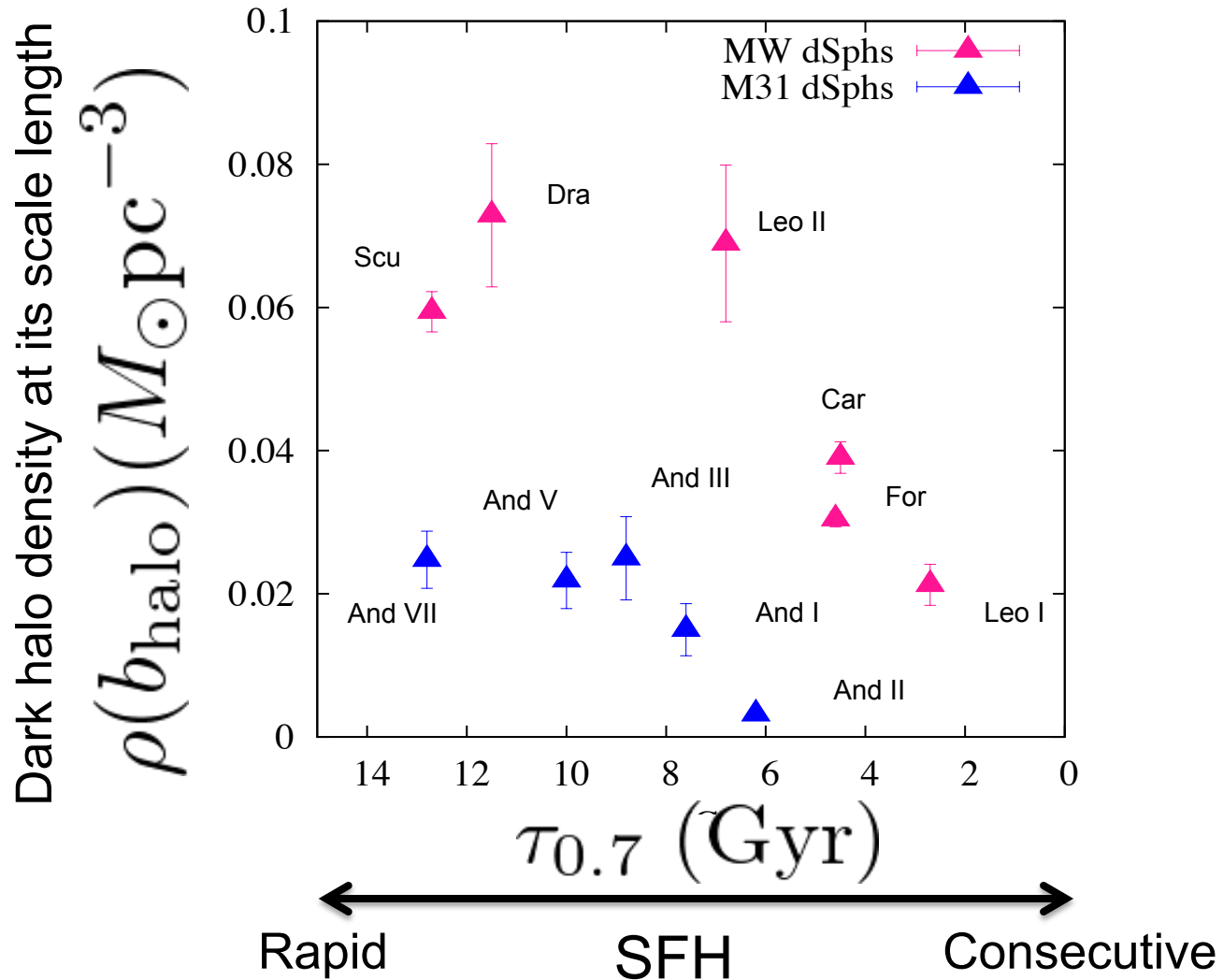
Characterizing the duration and efficiency of SF



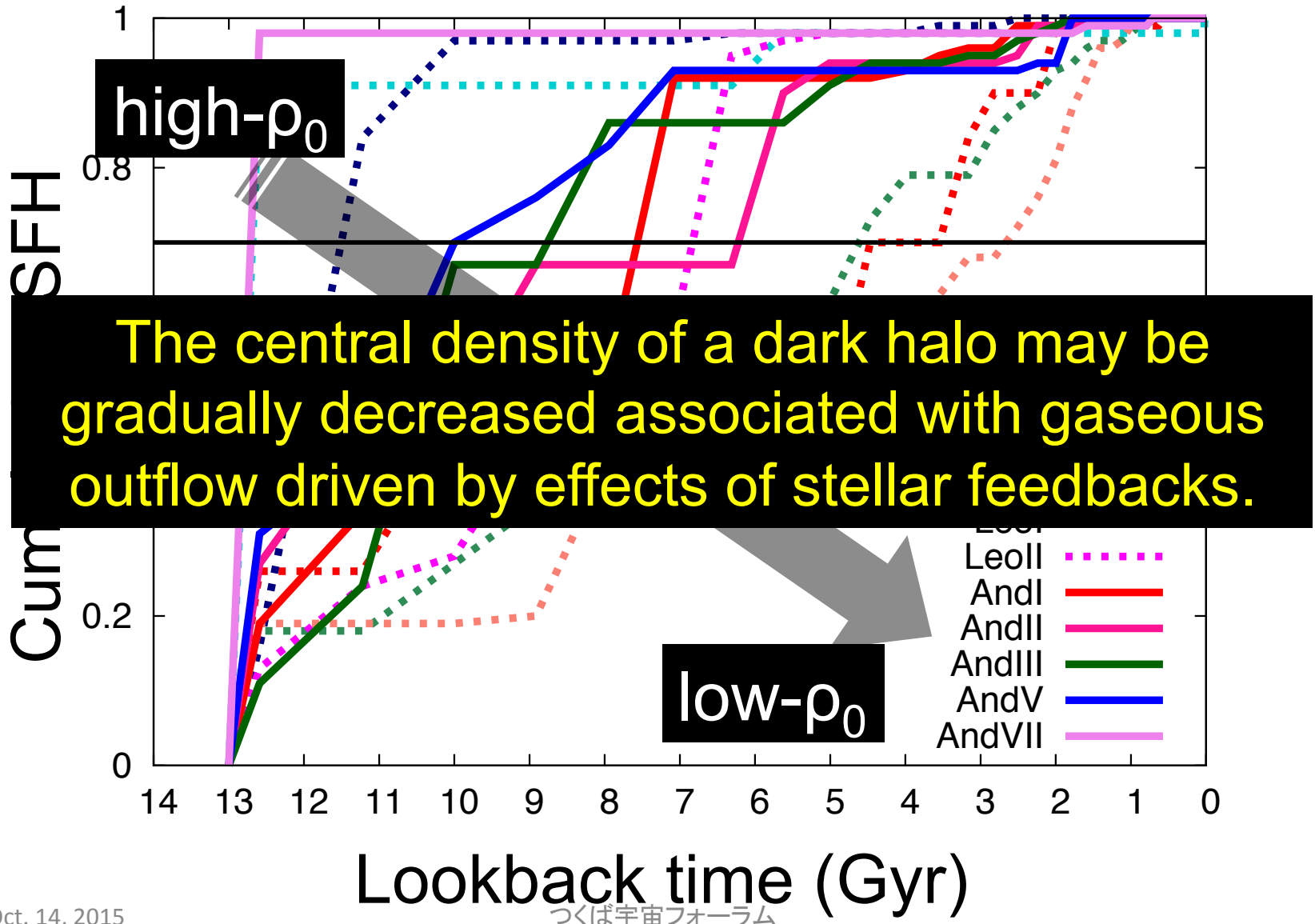
$\tau_{0.7}$ (horizontal line):

the lookback time at achieving 70% of current stellar mass of dSphs

The relation between DM halo & SFH



The relation between DM halo & SFH

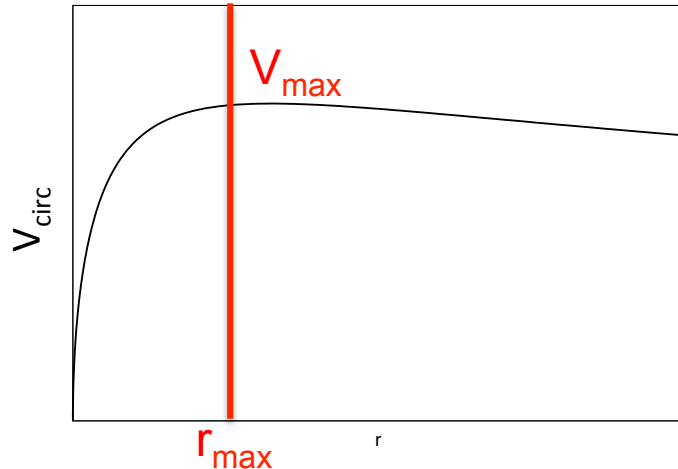


How cold is dark matter?

**: A CONSTRAINT FROM UNIVERSALITY OF DARK HALO
SURFACE DENSITY AT THE LOWEST HALO MASS SCALES**

Dark matter surface density within a radius of maximum circular velocity

- ✓ Maximum circular velocity



We suppose that a test particle perform circular motion in a DM halo potential.

$$V_{\text{circ}}(r) = \sqrt{\frac{GM(< r)}{r}}$$

r_{max} indicates the radius of the maximum value of circular velocity, V_{max} .

- ✓ DM surface density within r_{max}

$$\Sigma_{V_{\text{max}}} = \frac{M(r_{\text{max}})}{\pi r_{\text{max}}^2}$$

$$M(r_{\text{max}}) = \int_0^{r_{\text{max}}} 4\pi\rho(r')r'^2 dr'$$

Sample and assumed DM profiles

Galaxy type	Assumed DM profile	Reference
Late- and early-type spirals	pseudo-isothermal profile	de Blok+ 2008 Spano+ 2008
dwarf irregulars	Burkert profile	Gentile+ 2005, 2007
spirals and ellipticals	Burkert profile	Donato+ 2009
MW and M31 dwarf spheroidals	double power law (any slope) profile	KH & Chiba 2015b

$$\rho(r) = \frac{\rho_0}{\left[1 + \left(\frac{r}{r_0}\right)^2\right]^{3/2}}$$

pseudo-isothermal

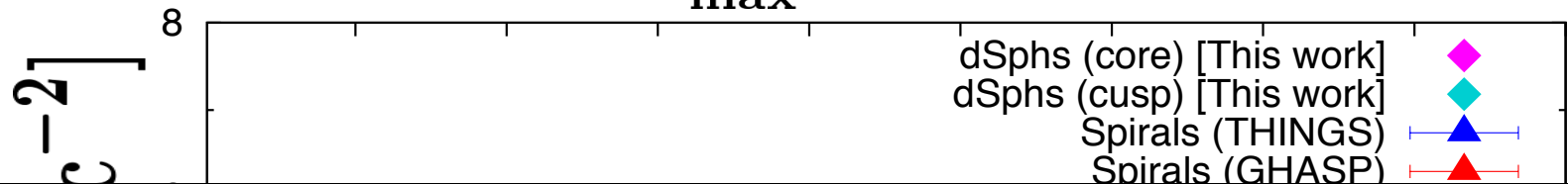
$$\rho(r) = \frac{\rho_0 r_0^3}{(r + r_0) (r^2 + r_0^2)}$$

Burkert

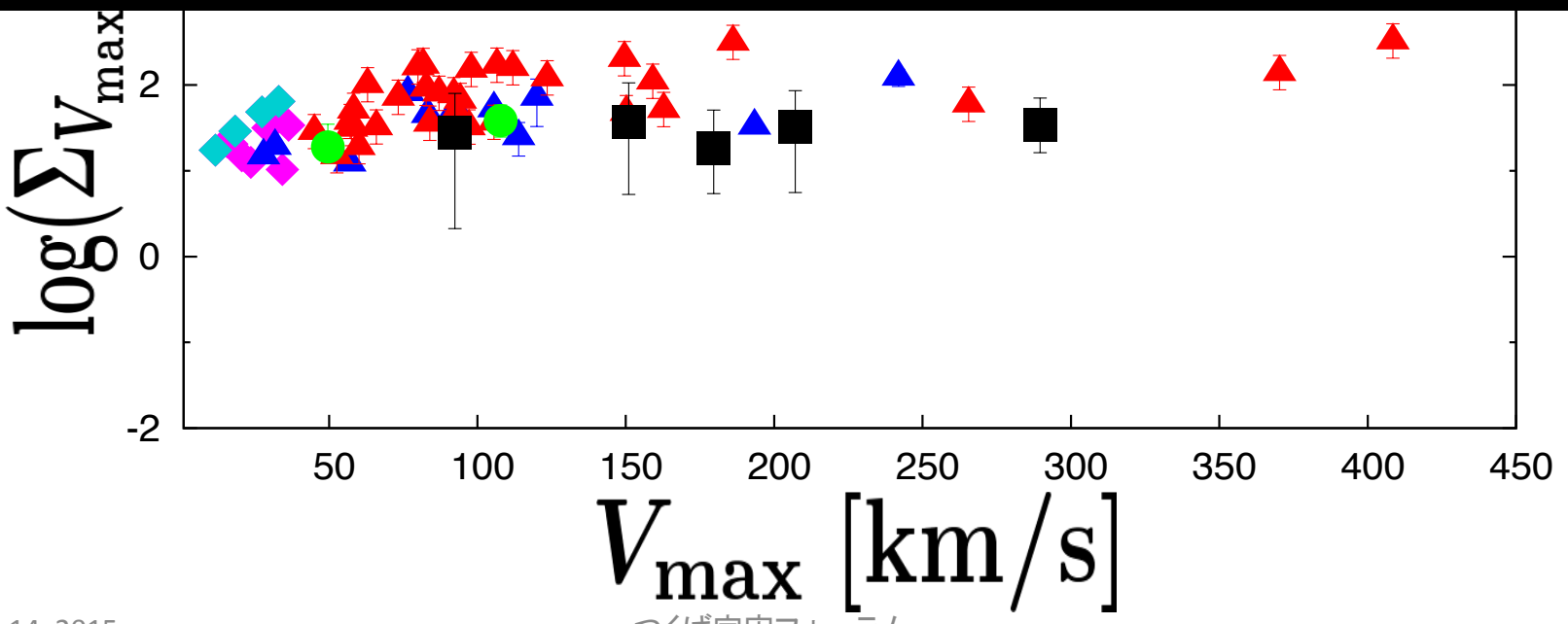
$$\rho(r) = \rho_0 \left(\frac{r}{r_s}\right)^\alpha \left[1 + \left(\frac{r}{r_s}\right)\right]^{-(\alpha+3)/2}$$

Double power-law

$$\Sigma_{V_{\max}} = \frac{M(r_{\max})}{\pi r_{\max}^2} \quad \text{vs.} \quad V_{\max}$$



Dark matter surface density within r_{\max} is almost constant across a wide range of galaxies, irrespective of dark halo density profiles.



DM surface density from CDM and WDM

- NEW DM density profile

$$\rho(r) = \frac{\rho_s}{(r/r_s)(1+r/r_s)^2}$$

- scale density and scale length

$$\rho_s = \frac{\rho_{\text{crit}} \Delta_m}{3} \frac{c^3}{\ln(1+c) - c/(1+c)}$$

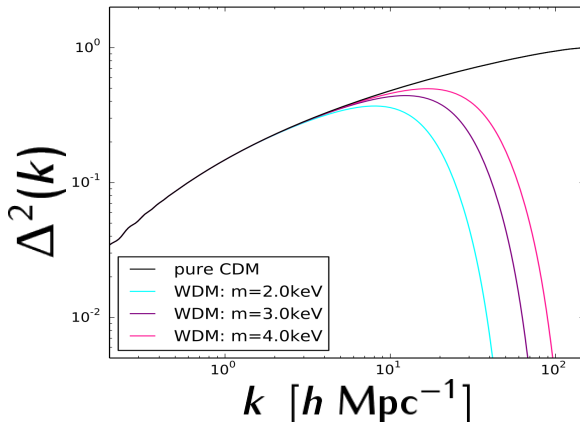
$$r_{\text{vir}} = \left(\frac{3M_{\text{vir}}}{4\pi\rho_{\text{crit}}\Delta_m} \right)^{1/3}$$

- DM surface density

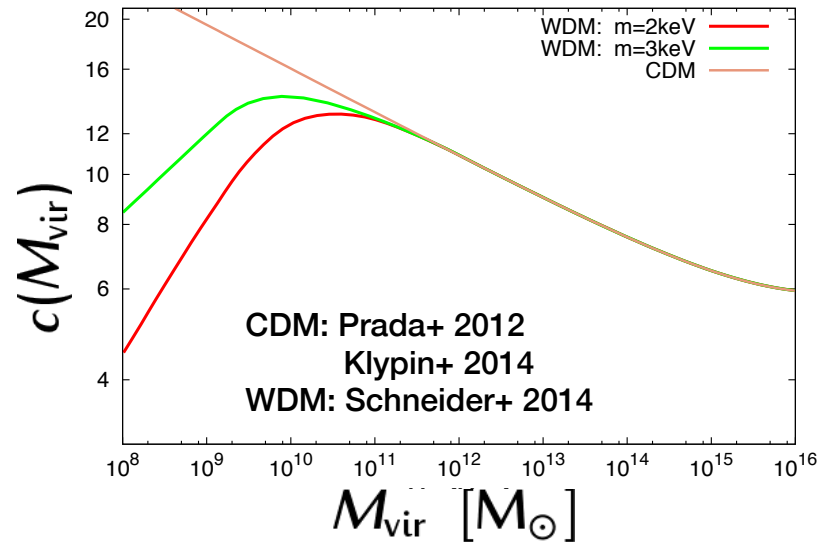
$$\Sigma_{V_{\max}} = \frac{M(r_{\max})}{\pi r_{\max}^2}$$

$$M(r_{\max}) = \int_0^{r_{\max}} 4\pi\rho(r')r'^2 dr'$$

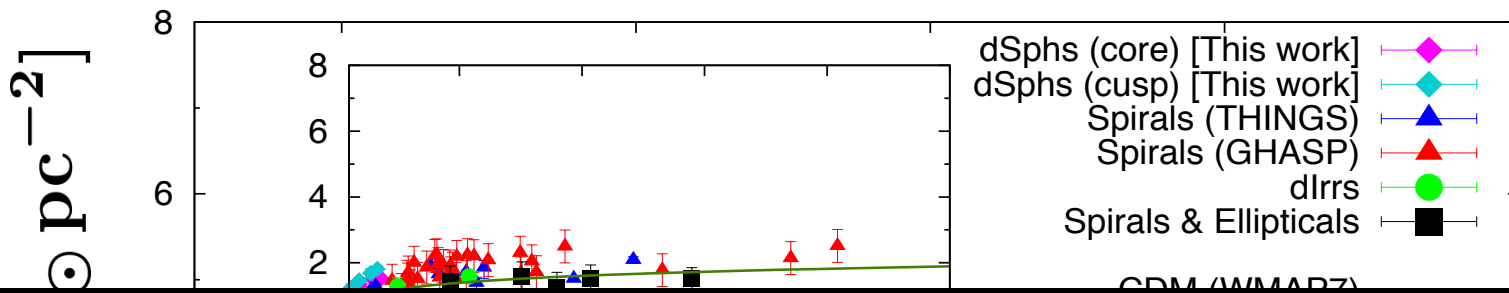
- Matter power spectrum



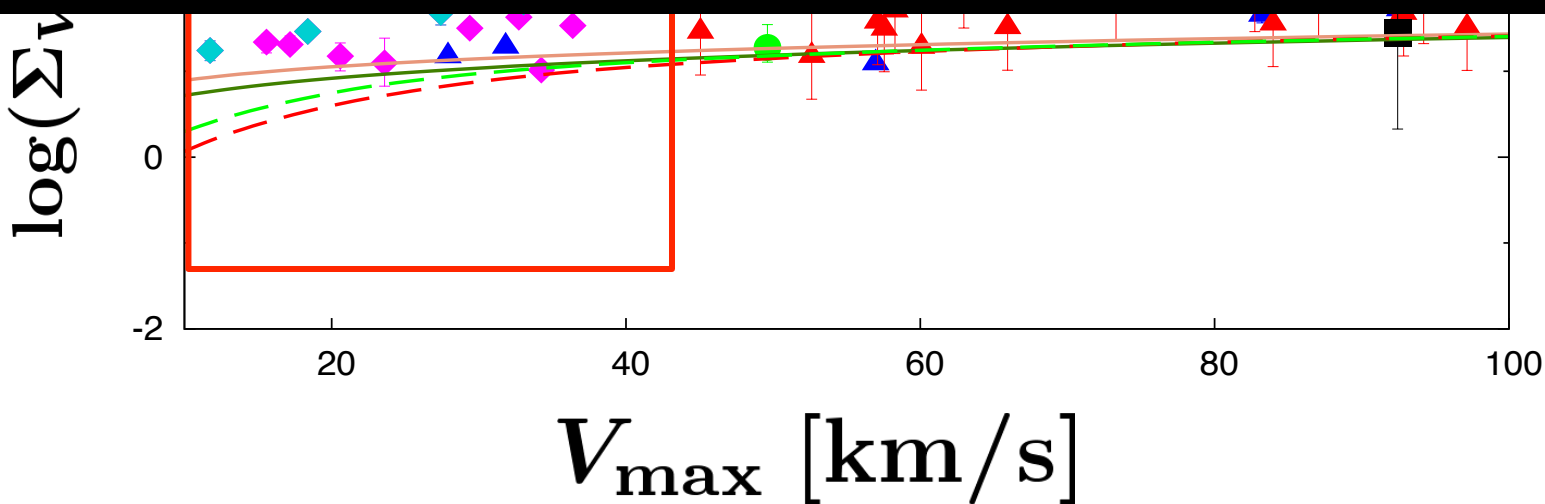
- Concentration parameter $c = \frac{r_{\text{vir}}}{r_s}$



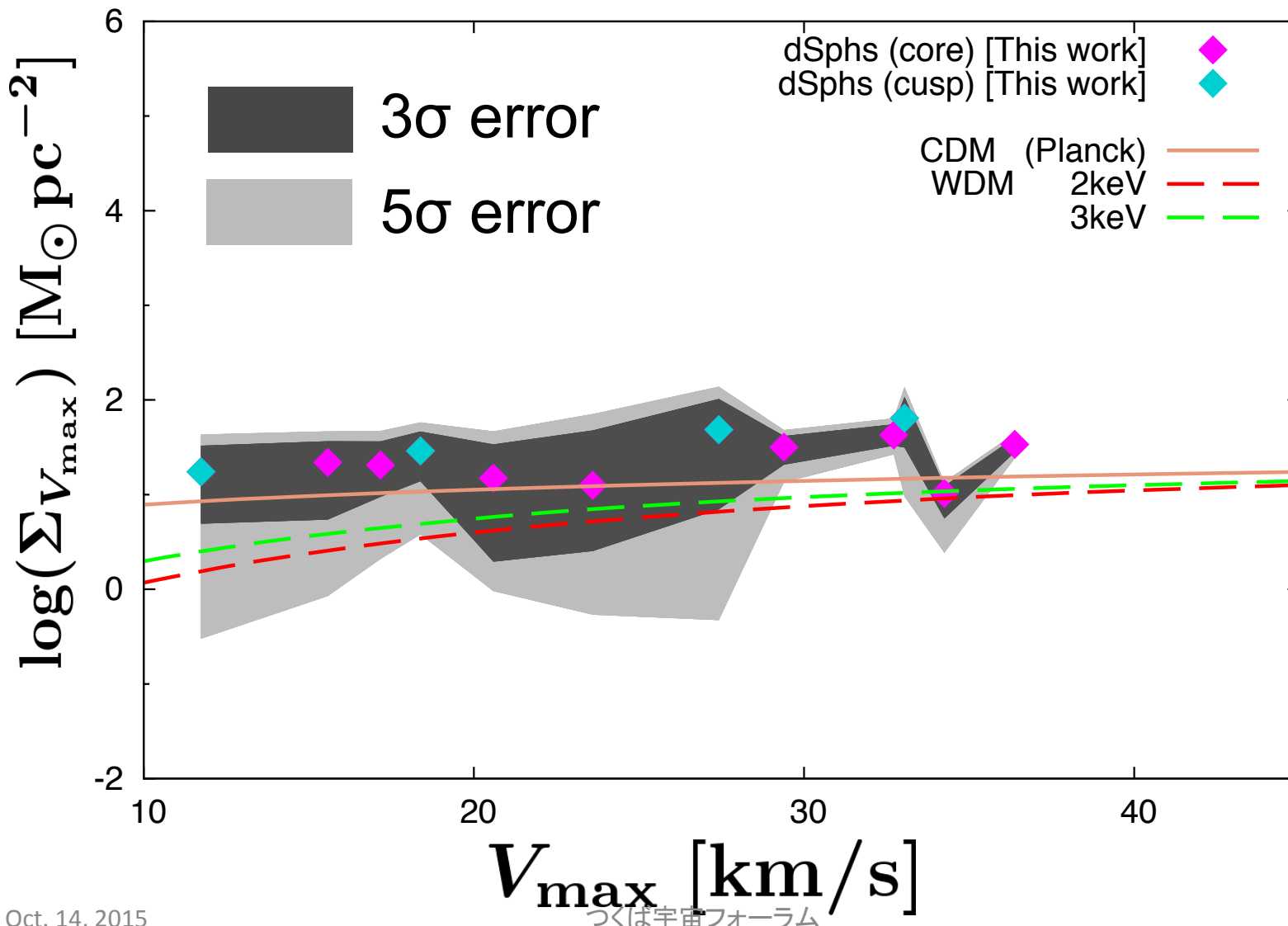
Comparison with dark matter scenario



Warm dark matter scenario
is inconsistent with this constancy.



How far do WDM deviate from data?



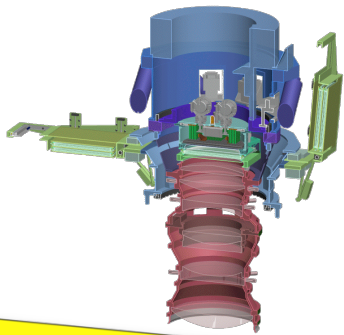
Summary

We have constructed axisymmetric mass models with velocity anisotropy for dSphs in the MW and M31 to obtain plausible limits on the structure of their dark halos.

- I. The best-fitting cases for most of the dSphs yield not spherical but flattened halos. These axial ratios are smaller than the CDM-based N-body predictions.
- II. The formation process of dSphs is intimately affected by the dynamical evolution of their dark halos and thus imprinted in their structures at the present time.
- III. It is found that dark matter surface density within a radius of V_{max} is nearly constant across a wide range of galaxies, and this universality is enable us to obtain the limits on particle masses of WDM scenario.
- IV. To set robust constraints on dark halo structures in dSphs, we require deep photometric data to assemble many sample stars down to faint magnitudes and spectroscopic data over large areas out to their tidal radii.

FUTURE PROSPECTS

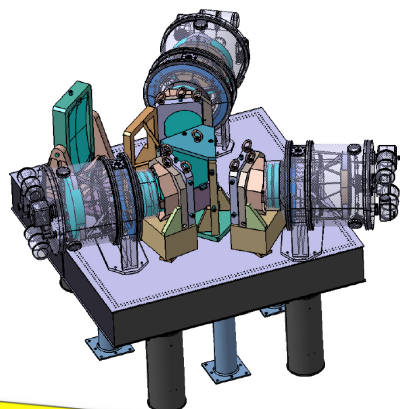
Future prospects



2014

Subaru/HSC

- Discovery of New UFD
- Hunting a number of faint stars in MW and M31 satellites



2018

Subaru/PFS

- Determining $[\alpha/\text{Fe}]$ and better radial velocities for many faint stars in MW dSphs via PFS with MR ($R \sim 5,000$).



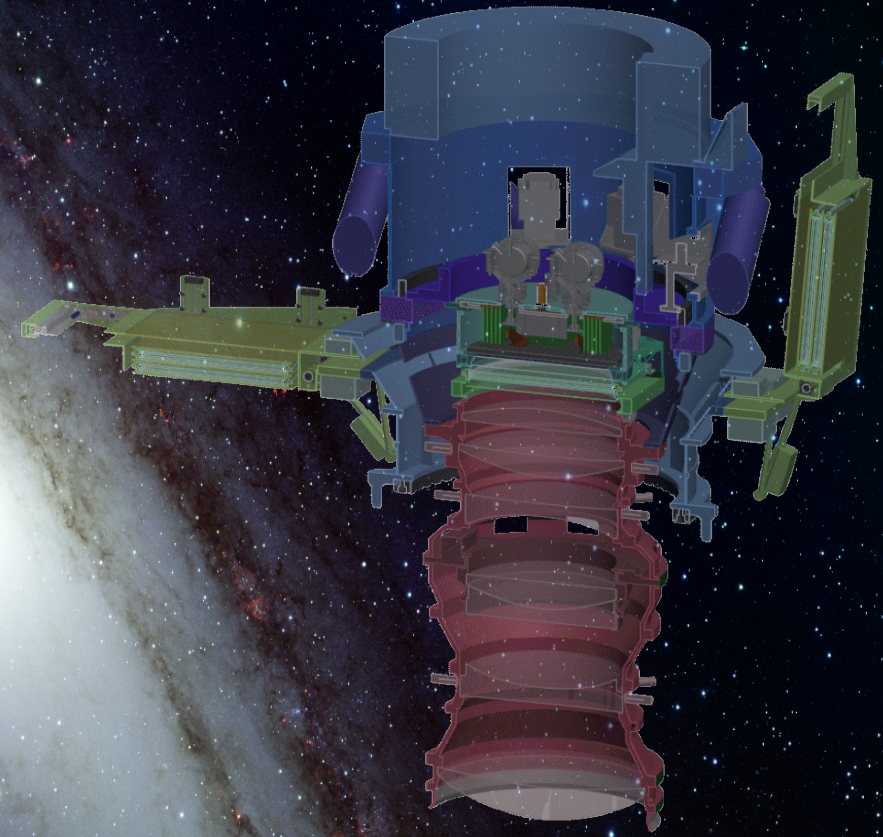
2020



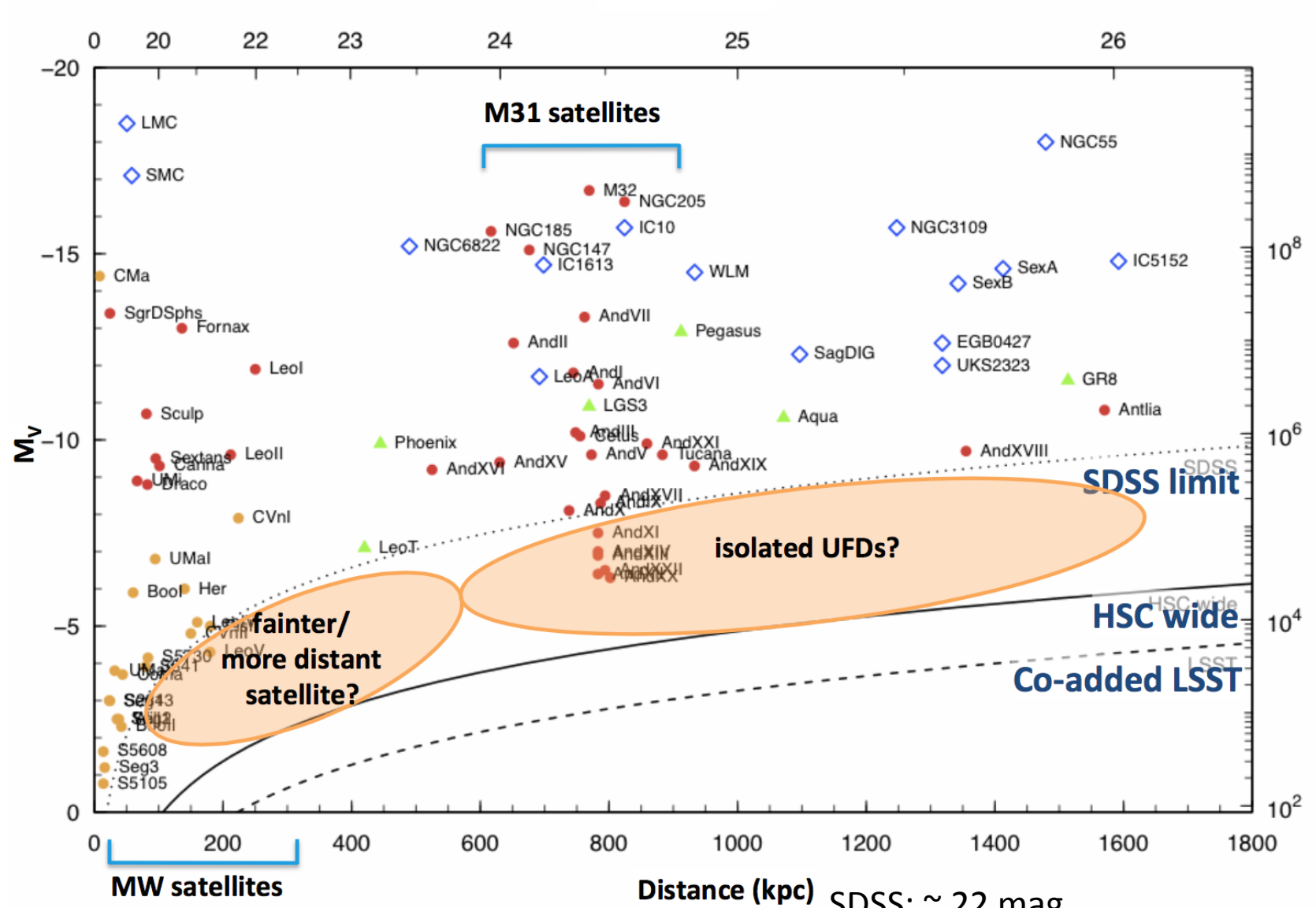
TMT

- Can obtain high-precision radial velocities of member stars via HROS ($R \sim 50,000$).

SUBARU HYPERSUPRIME-CAM

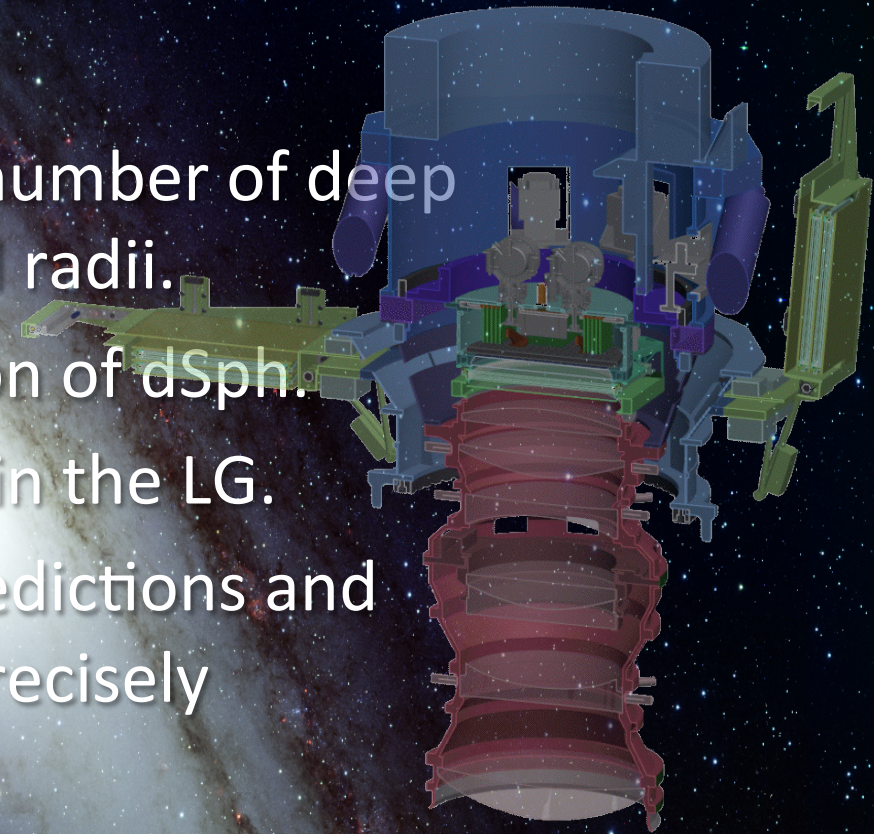


Search for NEW dSphs using HSC



SUBARU HYPERSUPRIME-CAM

- enables us to hunt a large number of deep photometric data over tidal radii.
- can unveil a true distribution of dSph.
- discover NEW faint dwarfs in the LG.
- compare between CDM predictions and observational facts more precisely

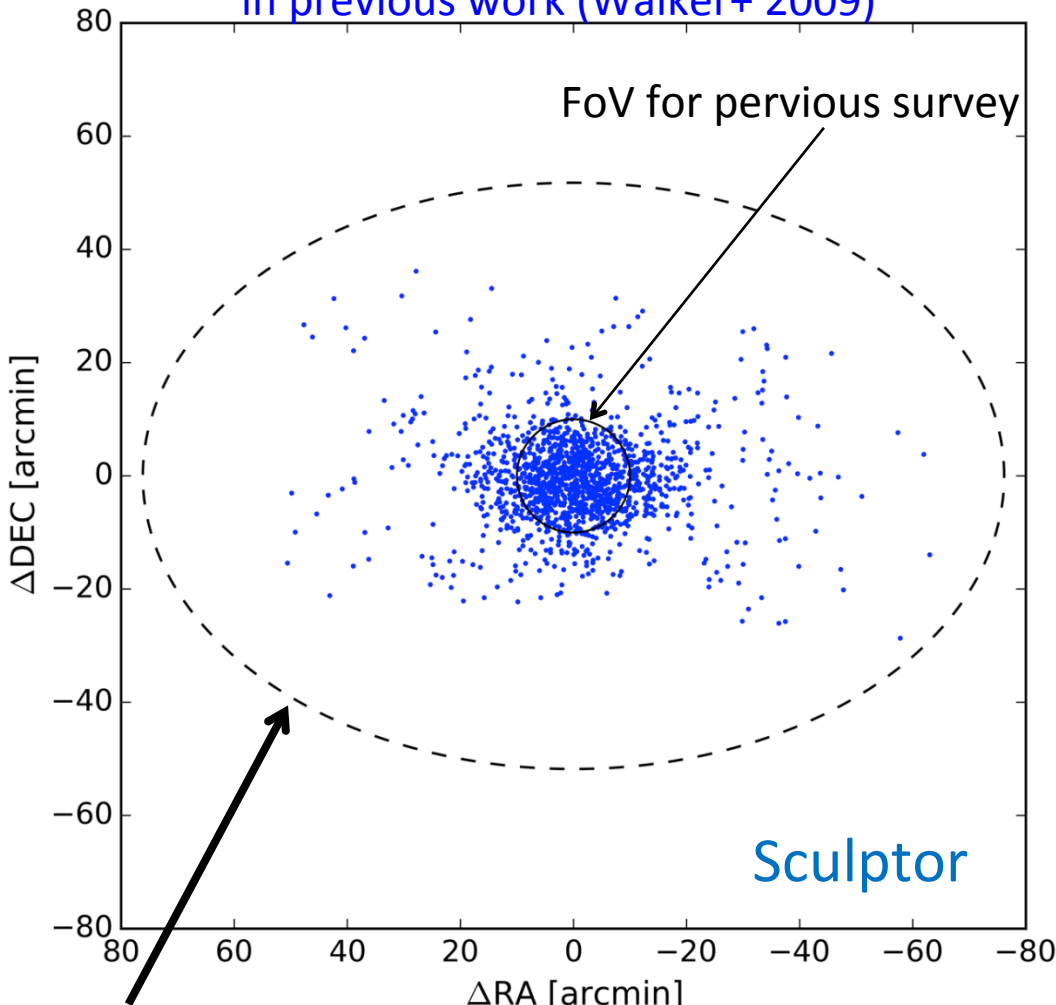


SUBARU PRIME FOCUS SPECTROGRAPH



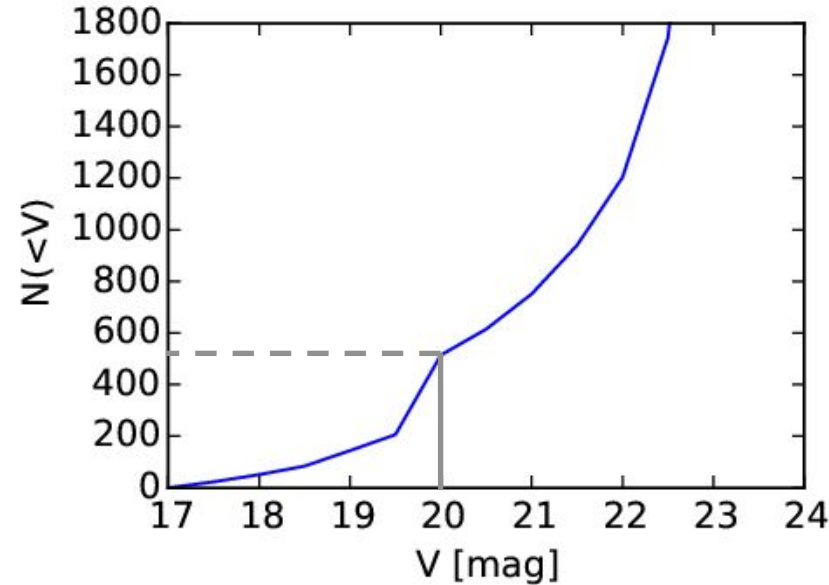
Wide & deep survey of MW dwarf galaxies w. Subaru/PFS

Blue dots: spectroscopic targets
in previous work (Walker+ 2009)



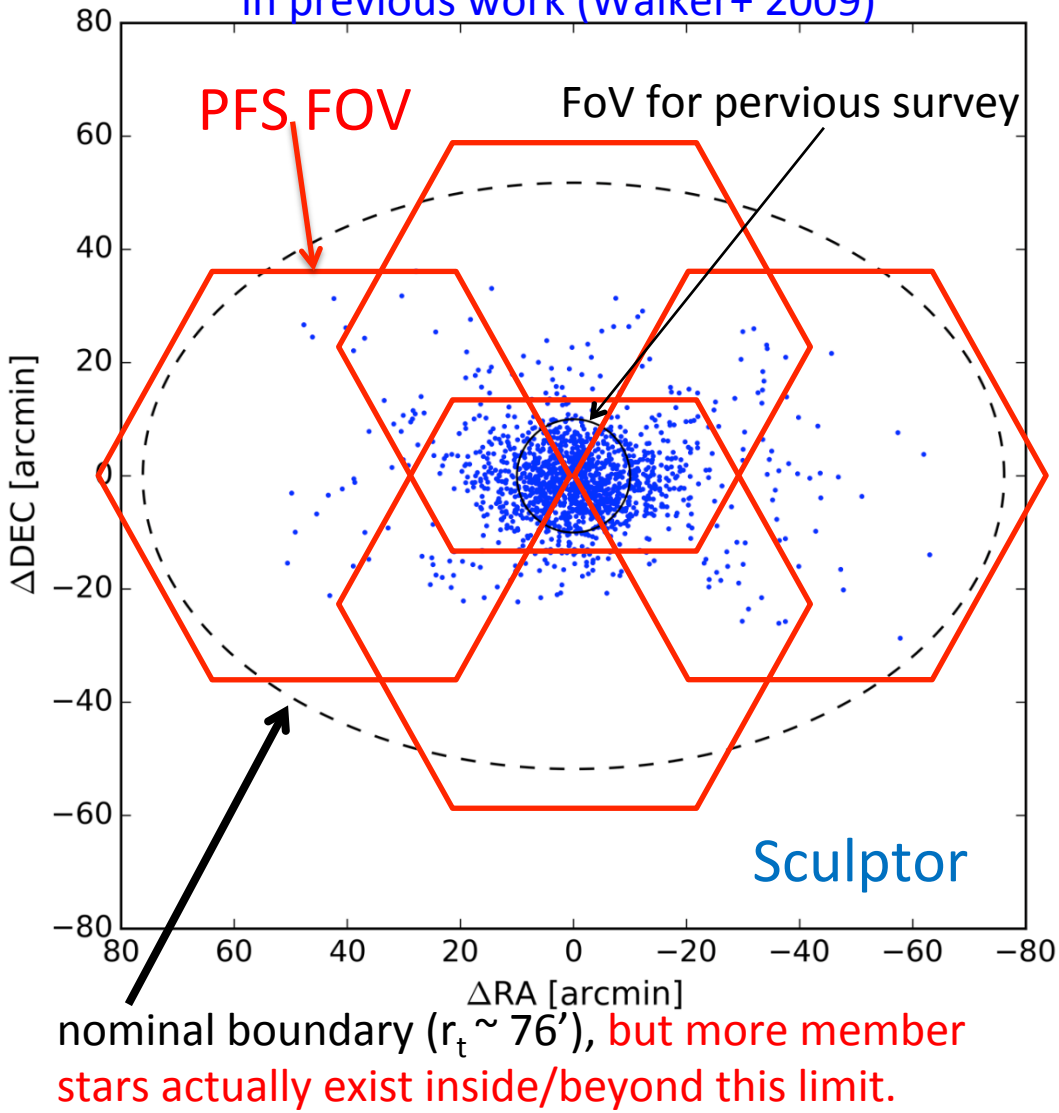
nominal boundary ($r_t \sim 76'$), but more member
stars actually exist inside/beyond this limit.

Cumulative number of observable stars
(previous work by Walker+ 2009)

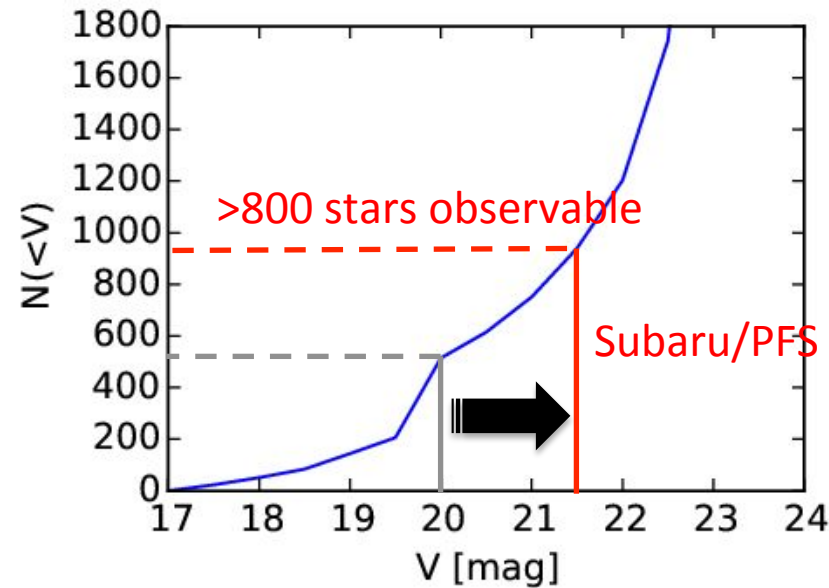


Wide & deep survey of MW dwarf galaxies w. Subaru/PFS

Blue dots: spectroscopic targets
in previous work (Walker+ 2009)



Cumulative number of observable stars
w. Subaru/PFS



Subaru/PFS enables us to measure
a large number of stellar spectra over
unprecedentedly wide outer areas,
where DM largely dominates!

⇒ Best for studying the nature of DM

SUBARU PRIME FOCUS SPECTROGRAPH

Subaru Prime Focus Spectrograph

- enables us to measure a large number of spectroscopic data over wide outer area.
- provides a better determination of dark halo properties of dSphs
- can obtain severer limits on the basic properties of dark matter.

THANK YOU FOR
YOUR ATTENTION!

FIN

LEM
4